ELEVATED-TEMPERATURE FRACTURE TOUGHNESS AND
FATIGUE TESTING OF STEELS FOR GEOTHERMAL APPLICATIONS

ANNUAL PROGRESS REPORT

DO NOT MICROFILM
COVER

by

R. A. Cutler
E. C. Goodman
R. V. Guest
R. R. Hendrickson
W. C. Leslie

Submitted to:

Brookhaven National Laboratory
Upton, Long Island, New York   11973

Attention: Dr. Daniel Van Rooyen

DOE Contract No. EY-76-C-02-0016

TR 80-87
November 1980

MASTER

TerraTek

DISCLAIMER

This report was prepared as an account of work sponsored by an agency of the United States Government. Neither the United States Government nor any agency Thereof, nor any of their employees, makes any warranty, express or implied, or assumes any legal liability or responsibility for the accuracy, completeness, or usefulness of any information, apparatus, product, or process disclosed, or represents that its use would not infringe privately owned rights. Reference herein to any specific commercial product, process, or service by trade name, trademark, manufacturer, or otherwise does not necessarily constitute or imply its endorsement, recommendation, or favoring by the United States Government or any agency thereof. The views and opinions of authors expressed herein do not necessarily state or reflect those of the United States Government or any agency thereof.

DISCLAIMER

Portions of this document may be illegible in electronic image products. Images are produced from the best available original document.

DOE/CH/00016--T2

ELEVATED-TEMPERATURE FRACTURE TOUGHNESS AND
FATIGUE TESTING OF STEELS FOR GEOTHERMAL APPLICATIONS

ANNUAL PROGRESS REPORT

DOE/CH/00016--T2

DE83 013874

by

R. A. Cutler
E. C. Goodman
R. V. Guest
R. R. Hendrickson
W. C. Leslie

Submitted to:

Brookhaven National Laboratory
Upton, Long Island, New York   11973

Attention: Dr. Daniel Van Rooyen

DOE Contract No. EY-76-C-02-0016

Submitted by:

Terra Tek, Inc.
University Research Park
420 Wakara Way
Salt Lake City, Utah   84108

TR 80-87
November 1980

ABSTRACT

Conventional drill bit steels exhibit increased wear and decreased toughness when run at elevated temperatures in geothermal wells. Bits are therefore run at lower speeds and lighter loads, resulting in lower penetration rates for geothermal wells than for conventional rock drilling.

Carpenter EX-00053, Timken CBS 600, Timken CBS 1000M and Vasco X-2M, steels with improved hot hardness (improved wear resistance), were tested in conjunction with the steels used for cones (AISI 4820 and 9315) and lugs (AISI 8620 and 9315) in conventional roller cone rock bits. Short-rod fracture toughness measurements were made on each of these steels between room temperature and 400°C. Fatigue crack resistance was determined at 300°C for high-temperature steels and at room temperature for conventional steels. Scanning electron microscopy analyses of the fractured short-rod specimens were correlated with observed crack behavior from the test records. Test results are discussed, recommendations made for further testing and preliminary steel selections made for improved geothermal bits.

i

TABLE OF CONTENTS

LIST OF ILLUSTRATIONS

LIST OF TABLES

INTRODUCTION

Current Geothermal Drilling Practice and Experience

Geothermal drilling is done almost exclusively with rolling cutter bits, 3-point stabilizers, and other conventional drilling equipment developed for oil and gas recovery, and for mining applications. Unfortunately these components have not been optimized for higher temperature operation, and deliver only about one-fifth of their normal life (footage) when used in some geothermal applications[1]. Performance in geothermal wells is further reduced since lighter bit loads must be used to prevent cataclysmic bit failures, and to avoid unwanted deviations caused by worn stabilizers. The resulting lower penetration rate (one-third to one-half of normal in many cases) is of much greater economic importance than the cost of the bit due to the high daily cost of the drill rig. A bit capable of doubling the penetration rate is worth eight times the cost of the conventional bit[2]. The time lost in "tripping" to replace the bit and stabilizers incurs high rig costs which exceed the cost of the replaceables by two to four times. The overall cost per foot can be reduced by 25 percent or more by the development of bits and stabilizers having service lives which are equivalent to those of conventional bits and stabilizers in nongeothermal use.

The most severe geothermal drilling environments are those involving air drilling into hot, hard, abrasive formations. Additional factors such as swelling, inclined bedding, and fractures can further slow the drilling process. Air drilling is necessary in highly fractured, subhydrostatic

reservoirs to avoid "lost circulation", and to avoid permanent quenching of steam vents. The air provides very little cooling of the bit and stabilizers because (a) it has usually been heated to the formation temperature by the time it arrives at the bottom, and (b) its specific heat is much lower than that of mud or water. Friction can heat localized areas of the bearings to temperatures far in excess of the formation temperature. Surface corrosion and stress corrosion cracking (hydrogen embrittlement) are generally insignificant in air-drilled geothermal wells. The drill bit is only exposed to steam as it passes through a steam entry point, or when tripping, since the drilling air provides a constant purging action. The H_2S embrittlement problem usually decreases with increased temperature, evidenced by the fact that brittle failure of drill bits at the Geysers has been almost non-existent[3].

Previous Terra Tek/DOE Geothermal Drill Bit Program Results

New steels and tungsten carbides for geothermal roller cone bits were evaluated by a combination of full-scale laboratory drilling tests under simulated geothermal conditions, field geothermal drilling, and material properties tests[3]. Three generations of bits were built and tested; the third-generation bits concluded successful field tests at the Geysers in September, 1978. These prototypes exhibited an improvement of 40 percent in bit life. The lack of suitable stabilizers precluded evaluation of higher bit weights, which would have demonstrated the full potential of the new bits.

The Drilling Research Laboratory, shown in Figure 1, was utilized for evaluation of all three generations of bits. The first two generations

TABLE 1

Wear Measurements for Conventional and MK-II Experimental Bits
Tested at 316°C in Geothermal Wellbore Simulator

	CONVENTIONAL BIT "A""	MK-II BIT "G"	MK-II BIT "H"
LOAD, POUNDS	20,000	25,000	20,000
RUN-TIME, MINUTES	150-180[3]	120	100
LUG WEAR[1]			
Friction Pin	0.012	0.002	0.000
Ball Race	0.030	0.016	0.040
Roller Race, IN[2]	0.044	0.004	0.007
Roller Race, OUT[2]	0.060	0.003	0.003
CONE WEAR[1]			
Friction Pin	0.001	0.001	0.000
Ball Race	0.018	0.000	0.004
Roller Race, IN[2]	0.025	0.006	0.007
Roller Race, OUT[2]	0.033	0.005	0.015

1. All wear measurements in inches; values shown are maximums.

2. Two measurements were made of tapered wear on both cones and bits.
   IN and OUT measurements are described in Figure 9 of Terra Tek
   Report TR 78-41.

3. Bit "A" ran for five hours and 16 minutes, but cones locked between 150-
   180 minutes into test, at which time wear on bearing surfaces would have
   stopped.
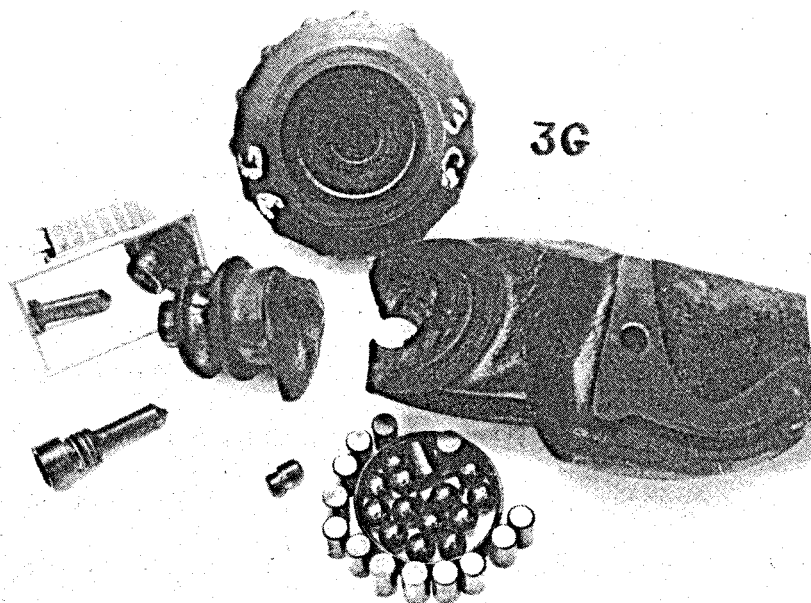
Figure 4. Brittle failure of H-13 lug.

Steels were sought for the third generation bits which could maintain high levels of fracture toughness in addition to maintaining high hardness in the bearing races and high tensile strength to prevent rupture. Baseline fracture toughness tests on AISI 8620 (conventional lugs) and AISI 4820 (conventional cones) indicated toughness values of 135 MPa$\sqrt{m}$ (123 ksi$\sqrt{in}$)* and 90 MPa$\sqrt{m}$ (82 ksi$\sqrt{in}$) respectively. Steels were sought for the lugs and cones which could meet these fracture toughness requirements, with the best attainable race hardness values. The materials selections are shown in Figure 5. Laboratory determinations of fracture toughness for M50 (rollers), shown in Figure 6, illustrate how some hardness was sacrificed to maximize fracture toughness. It is important to realize that the sacrifice of hardness does not always enhance the toughness of steels. Figure 7 plots fracture toughness as a function of temperature for the CBS 600 lug steel; these data were obtained using the "short-rod" technique with 2-inch diameter by 3-inch long samples. It should be noted that toughness decreases with temperature for this steel, thus illustrating the importance of elevated-temperature toughness testing: all previously tested steels exhibited increasing toughness with temperature. Figure 8 shows the desirable hot-hardness characteristics of CBS 600, as compared to AISI 8620.

Six of the third-generation bits were run at the Geysers by Union Geothermal; the prototypes were alternated with the Reed Y73-JA conventional bits which are geometrically identical. The bits drilled typical Geysers ("Franciscan") graywacke sandstone; the air entering the bits was

---

* The 1-inch diameter sample used for the AISI 8620 was too small for a valid K_{Ic} measurement, even with the "short-rod" method employed; the 135 MPa$\sqrt{m}$ figure is accurate to within ±15 percent.
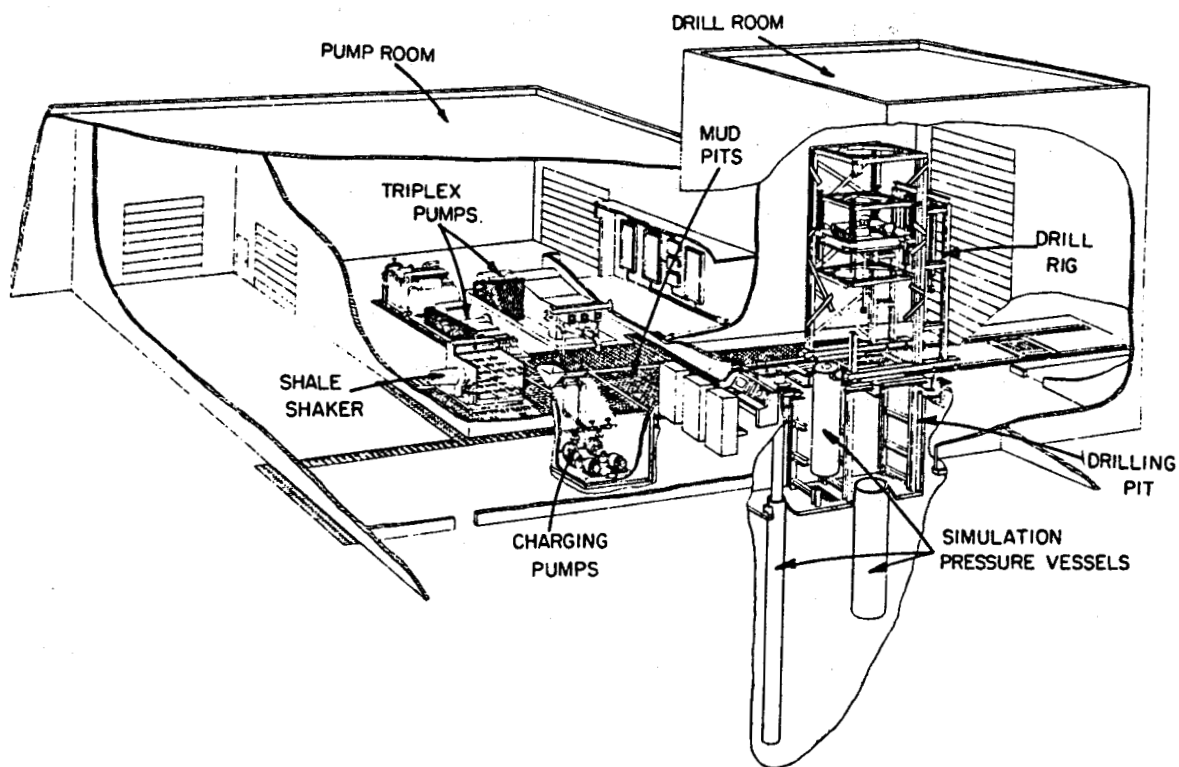
Figure 1. The Drilling Research Laboratory.

were run in the Geothermal Wellbore Simulator (Figure 2), while two of the third-generation bits were run in the Geothermal Air-Drilling Test Facility (Figure 3) prior to the field tests. A total of six third-generation bits were evaluated at the Geysers by Union Geothermal Division of Union Oil Company.

The first two generations of bits were fabricated by Reed Tool Company from tool steels which were known to retain hardness at temperatures to 400°C, such as H-13 (lugs), Vasco MA and Vasco X2 (cones), and M50 (bearings). Back-to-back drilling tests with conventional bits in the Geothermal Wellbore Simulator at 316°C revealed an approximate ten-to-one reduction in bearing wear (Table 1). While these results clearly indicated the importance of retaining bearing race hardness at temperature, brittle failures of both cones and lugs were experienced as shown in Figure 4.

3

PRESSURE VESSEL

INSULATION

HEATERS

STANDARD SIZE
17.15 cm (6 3/4") ROCK BIT

MILD STEEL DRILL PAD
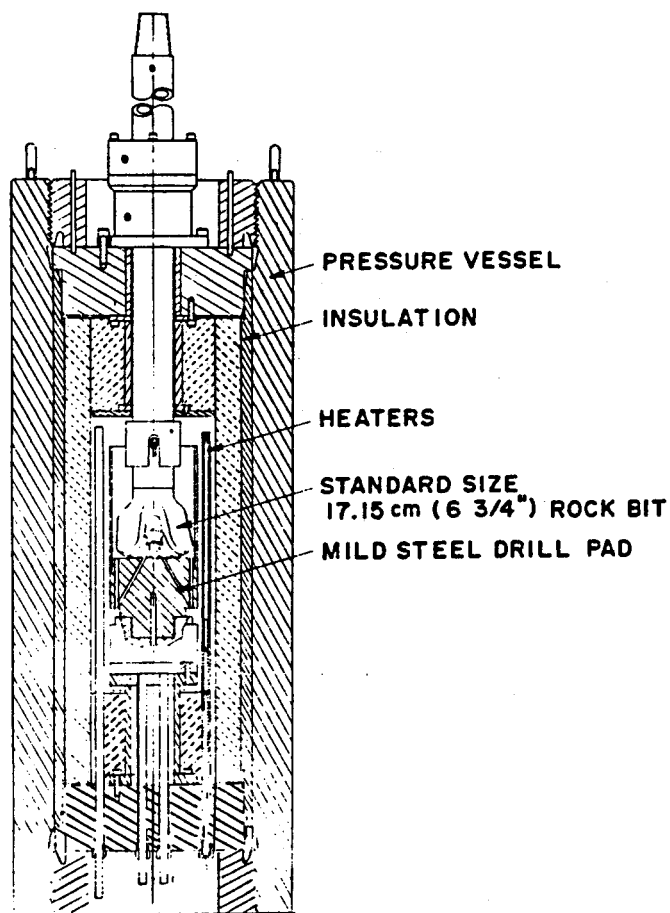
Figure 2.   Geothermal wellbore simulator.
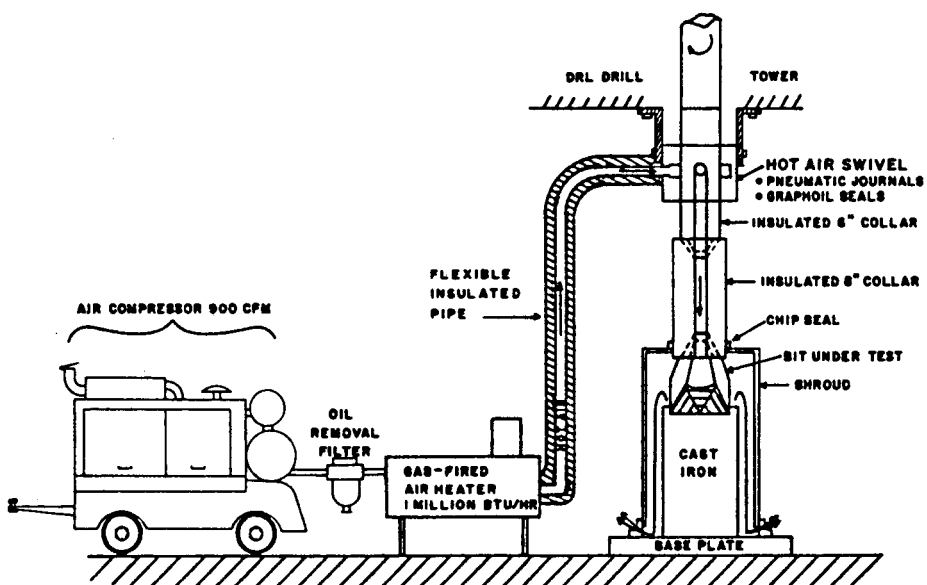
Figure 3.   The geothermal air-drilling test facility.

4

LUGS: CBS-600
STEEL (TIMKEN)

GAGE-ROW INSERTS:
CARBOLOY #90

REMAINING INSERTS:
CARBOLOY #231

ROLLERS AND BALLS:
M-50 STEEL AT
R_C-56

CUTTER CONES:
4820 STEEL

FRICTION-PIN
BUSHING:
CARBOLOY #248
OR M-50 STEEL
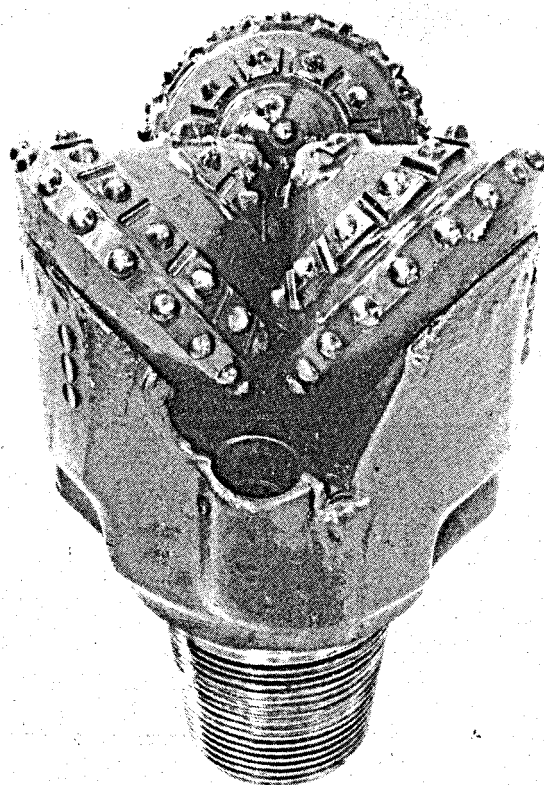
Figure 1. Materials selected for the third-generation drill bits.

7
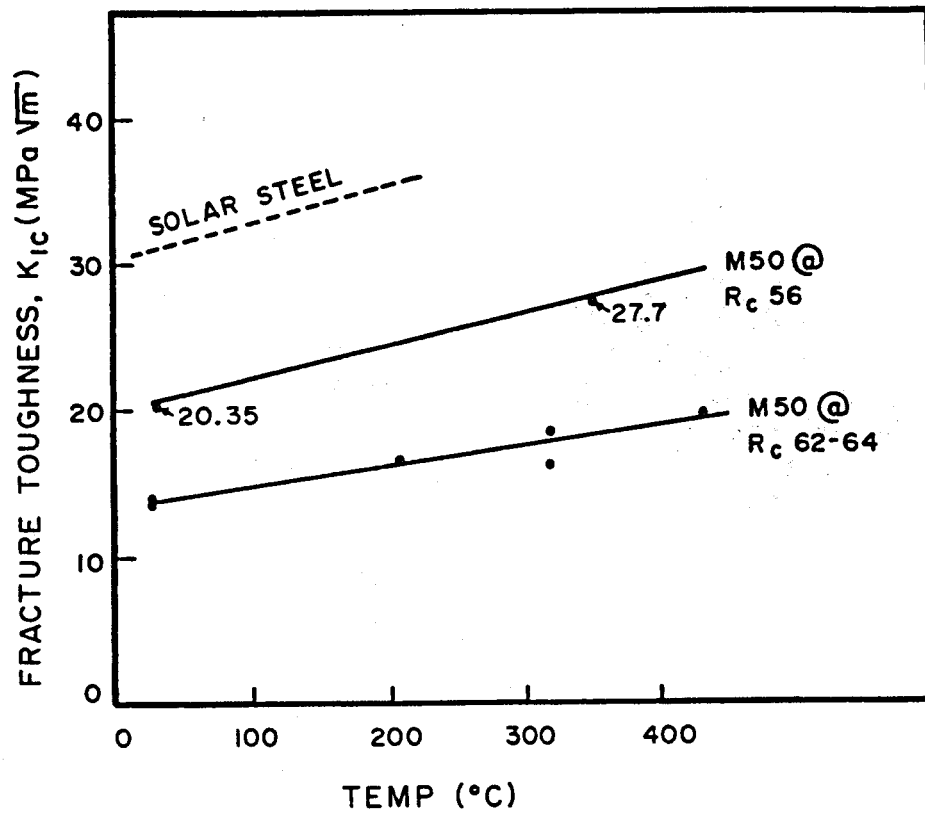
Figure 6. Fracture toughness for the roller bearing steels.
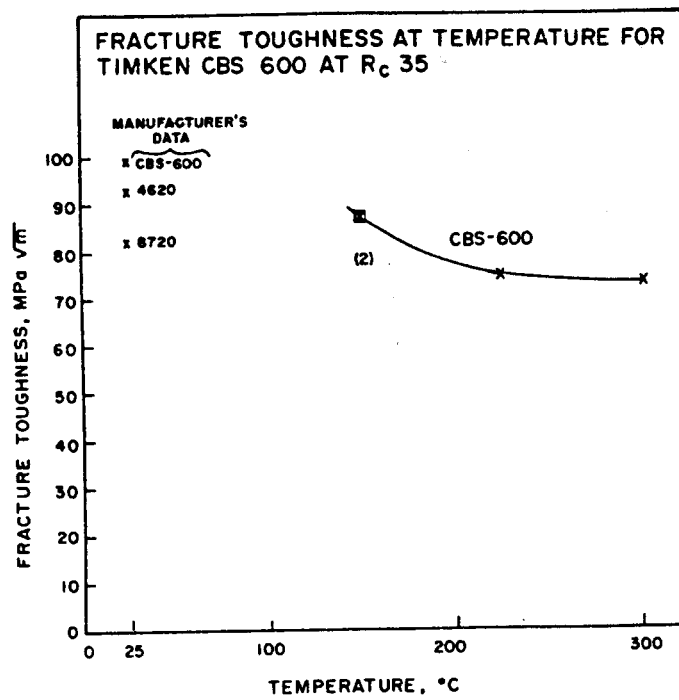
Figure 7. Fracture toughness at temperature for CBS 600 lug steel at a core hardness level of R_c35.
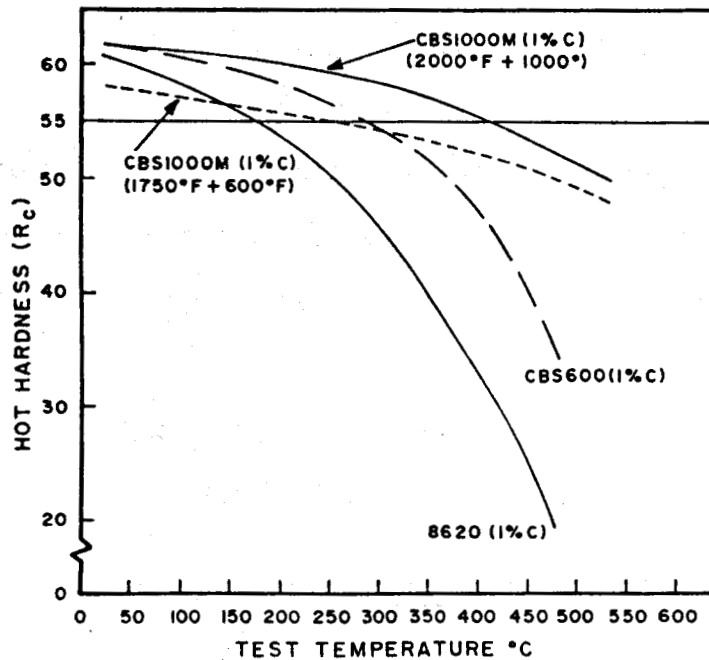
Figure 8. Hardness versus temperature for bit lug materials (Timken Corporation).

at the formation temperature, *i.e.*, about 240°C. A detailed post-mortem wear analysis (Figure 9) of the experimental and conventional bits revealed the superior performance of the third-generation bits.

The following conclusions and observations on bearing wear were drawn from these drilling tests[3]:

- The use of CBS 600 reduced lug wear by about 2½ to 1 in the ball and roller races, and on the pilot pins of the bits utilizing M50 bushings. Lug wear, although greatly improved, needs to be reduced further. Microhardness traces on sections of CBS-600 lugs indicated that surface temperatures exceeded 400°C on the roller and ball races, and 600°C under the Stellite on the end of the pilot pin. Deformation of the pilot pins was noted on the experimental bits but to a lesser extent than on the Y73JA's.

9

- CBS 600 should also be used for the cones.

- The M50 rollers experienced very minimal wear.

- The excessive ball wear was due to the design of the ball retainer plug; a definitive test of the M50 balls is still required. Good performance is expected, based on the low wear experienced by the M50 rollers.

- Overall wear in the pilot bearing system ("friction pin area") is excessive and should be reduced by a factor of three.
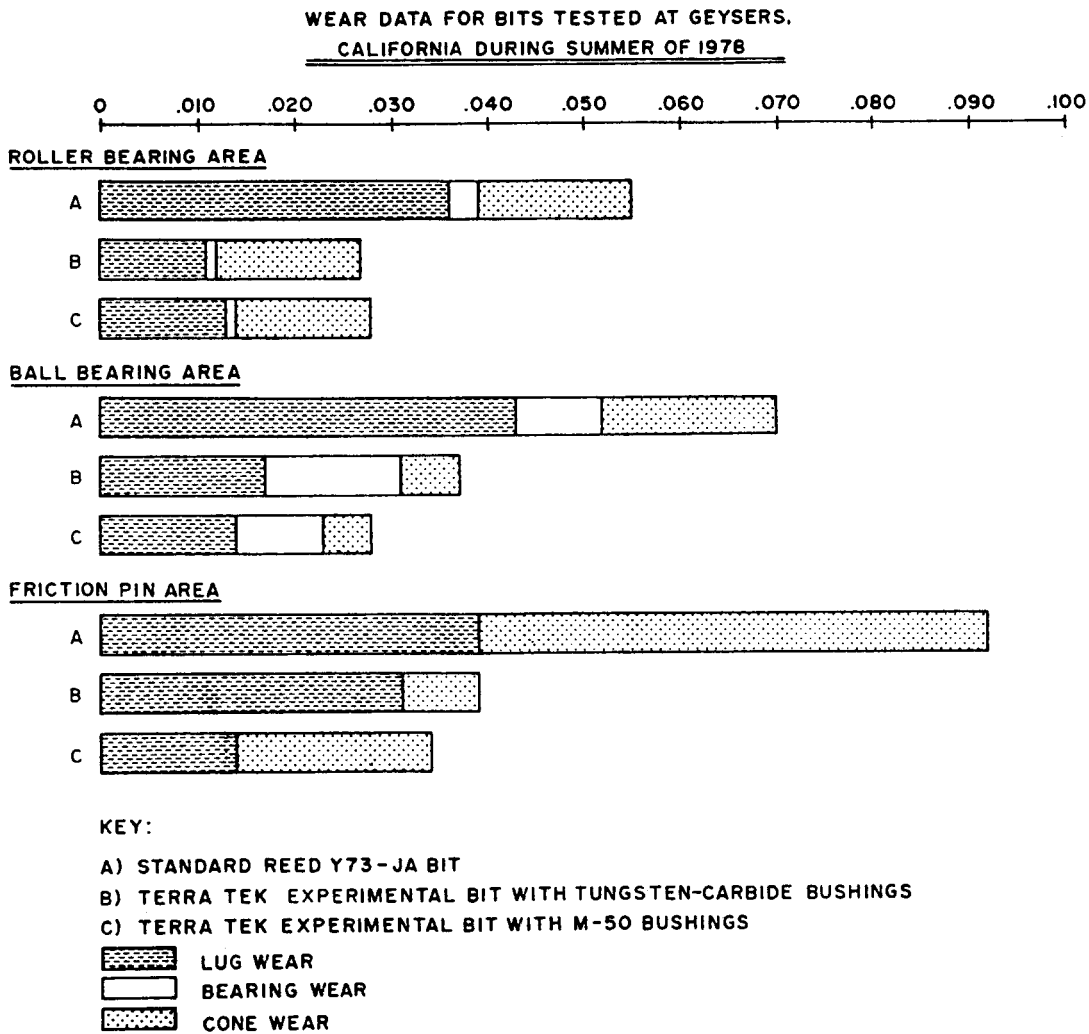
Figure 9. Wear data for bits tested at Geysers.

10

Current Research

The previous Terra Tek/DOE work greatly enhanced the understanding of the relationships between laboratory materials property tests and field drilling performance in the geothermal environment. Since conventional steels fail by excessive wear rather than by brittle fracture in the field[3], it was determined that steels which have high hot hardness and hence superior resistance to wear at elevated temperatures should be the prime candidates for improved geothermal lugs and cones. The brittle fracture of the cones and lugs of the MK-II experimental bits, however, indicate the need for fracture toughness and fatigue crack resistance in the experimental steels at levels comparable to those of the conventional steels. Three new candidate steels are listed in Table 2 along with CBS-600, which requires further evaluation.

TABLE 2

Candidate High-Temperature Alloy Steels

MANUFACTURER	ALLOY	RECOMMENDED BY
Carpenter	EX-00053	Smith Tool Company
Teledyne-Vasco	X2 Modified	Terra Tek/DOE Program
Timken	CBS 1000M	Timken Research Center
Timken	CBS 600	Terra Tek/DOE Program

11

All of these steels are either in use, or under consideration, for applications where high-strength, high-temperature carburizing steels are required. These include: helicopter main drive gears, speed reducers for turboprops, jet helicopters, and gas-turbine truck engines, as well as afterburner and thrust reverser mechanisms for military aircraft. Nominal composition for the high-temperature steels and for conventional steels are given in Table 3. Hardness of both the carburized case and core of all of these steels except AISI 4820 are displayed in Figure 10 as a function of temperature. The hardness of 8620 and 9315 declines rapidly with increasing temperature in both the case and core as opposed to the excellent retention of hardness in the experimental steels. Although manufacturer's hot-hardness data were not available for 4820, it is expected to behave similarly to 9315. CBS 1000M appears to have the highest hot-hardness.

The objectives of the present research are therefore to characterize the fracture toughness and fatigue behavior of steels presently used in rotary drill bits and reaming stabilizers and to identify high wear-resistance steels with equivalent toughness and fatigue crack resistance at temperatures to 400°C. It is felt that wear-resistant steels with fracture toughness values at 200°C-400°C between 90 MPa$\sqrt{m}$ (82 ksi$\sqrt{in}$) and 135 MPa$\sqrt{m}$ (123 ksi$\sqrt{in}$) would have sufficient toughness to maintain high penetration rates in geothermal wells. The 90-135 MPa$\sqrt{m}$ range was determined from a limited data bank of fracture toughness data for 4820 (cones) and 8620 (lugs) developed at Terra Tek[3]. The two steels which exhibited brittle failure in the MK-II bits had K_{Ic} values between 25 and 65 MPa$\sqrt{m}$ at temperatures up to 400°C[4].

TABLE 3

Nominal Steel Compositions

Steel Type	Composition (% by weight)										
	C	Mn	P	S	Si	Cr	Ni	Mo	V	W	Cu
AISI 4820	0.20	0.60	0.035	0.040	0.28	--	3.50	0.25	--	--	--
AISI 8620	0.20	0.80	0.035	0.040	0.28	0.50	0.55	0.20	--	--	--
AISI 9315	0.15	0.55	0.025	0.025	0.28	1.20	3.25	0.12	--	--	--
CBS 600	0.20	0.55	--	--	1.05	1.45	--	1.00	--	--	--
CBS 1000M	0.13	0.50	--	--	0.50	1.05	3.00	4.50	--	--	--
EX-00053	0.10	0.35	--	--	1.00	1.00	2.00	3.25	0.10	--	2.00
Vasco X2M	0.13	0.25	--	--	1.00	5.20	0.06	1.30	0.40	1.35	--
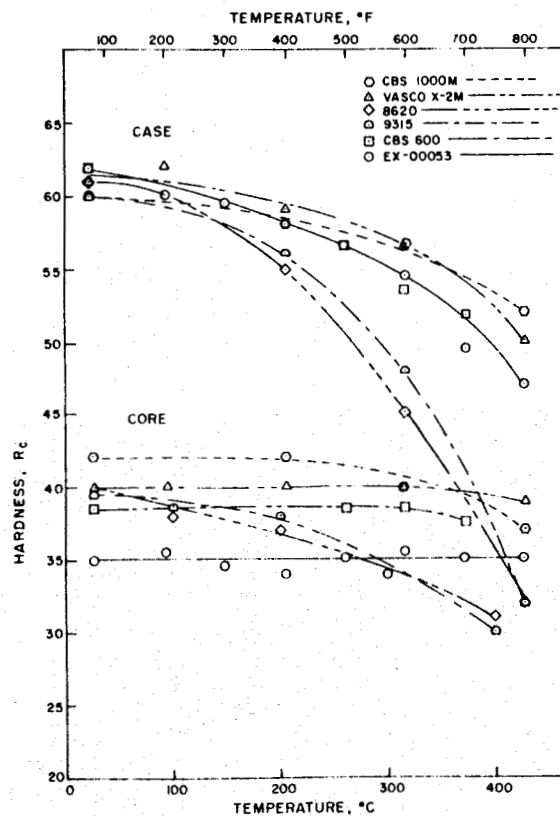
Figure 10. Effect of temperature on hardness of conventional and experimental steels.

EXPERIMENTAL PROCEDURE

Sample Preparation

AISI 4820: Test blanks 50.8 mm diameter by 76.2 mm long were machined from a forged and annealed rod 1.8 m in length. The steel was of aircraft quality and had been vacuum melted. The long axes of the blanks were parallel to the axis of forging.

AISI 8620: Cylinders 50.8 mm diameter by 76.2 mm long were made from an air-melted, hot-rolled rod 57.2 mm diameter by 1.8 m in length. The long axes of the specimens were parallel to the rolling direction.

AISI 9315: Specimens 25.4 mm diameter by 38.1 mm long were cut from aircraft-quality, vacuum-arc-remelted steel. The hot-rolling direction was parallel to the long axes of the cylinders.

CBS 600: Cylindrical rods 50.8 mm diameter by 76.2 mm long were machined from vacuum-arc-remelted, hot-rolled stock. The long axes of the specimens were parallel to the rolling direction. Test blanks 25.4 mm diameter by 38.1 mm long were made from a forged bar which was quartered before machining the diameter of the cylinders. The long axes of the specimens were again parallel to the axis of forging.

CBS 1000M: Test blanks 50.8 mm diameter by 76.2 mm long were turned from a hot-rolled 76.2 mm diameter rod. The steel had been vacuum induction melted and vacuum-arc-remelted (VIMVAR) and specimen axes were parallel to the rolling direction. 25.4 mm diameter by 38.1 mm long cylinders were made from a separate heat in an identical manner except that the steel was rolled to the smaller diameter.

EX-00053: A rough forged rod approximately 60 mm in diameter was machined into cylinders 50.8 mm diameter by 76.2 mm long. The steel was VIMVAR and specimen axes were parallel to the axis of forging.

X-2M: Vacuum-melted, hot-rolled rods were used to make cylinders 50.8 mm diameter by 76.2 mm long. The cylinder axes were parallel to the rolling direction.

Ladle analyses of 4820, 8620, EX-00053 and X-2M, as well as the chemical composition of the 25.4 mm cylinders supplied by the Timken company, are listed in Table 4. Detailed heat treatments of each of the steels appear in Appendix A. A grip groove was machined into the end of each specimen as illustrated in Figure 11. Thin slots were then machined longitudinally in the cylinder, leaving a "V"-shaped ligament in the intended crack plane.

Testing and Data Reduction

Fracture Toughness: The short-rod method[5] was used to measure the fracture toughness of the steels as a function of temperature. The theory for this novel technique has been developed for materials displaying linear elastic fracture mechanics (LEFM)[6] and for non-LEFM specimens[7]. Comparisons of the short-rod technique with the standard ASTM E399 method of measuring fracture toughness have shown good agreement[8], as have different techniques for calibrating the short-rod specimens[9,10]. Although several advantages of the short-rod method have become apparent[11], the main reason for using the technique to evaluate drill bit materials is that specimen diameters similar to the through-section thickness of cones or lugs can be

TABLE 4

Ladle and Check Analyses of Steels

Steel Type	C	Mn	P	S	Si	Cr	Ni	Mo	V	W	Cu	Al
AISI 4820[1]	0.18	0.65	0.012	0.013	0.26	0.15	3.30	0.25	--	--	0.08	--
AISI 8620[1]	0.19	0.74	0.013	0.021	0.21	0.48	0.47	0.18	--	--	0.04	0.050
AISI 9315[2]	0.13	0.59	0.009	0.006	0.31	1.31	3.28	0.12	--	--	--	0.030
CBS 600[2]	0.20	0.60	0.004	0.004	1.01	1.55	0.06	0.97	--	--	--	0.036
CBS 1000M[2]	0.13	0.54	0.008	0.007	0.38	1.01	3.05	4.47	0.39	--	--	0.035
EX-00053[1]	0.103	0.33	0.007	0.006	0.95	0.99	2.03	3.32	0.11	--	2.06	--
X-2M[1]	0.14	0.20	0.014	0.003	0.98	4.80	--	1.33	0.45	1.34	--	--

[1] Ladle analysis

[2] Chemical composition of test cylinders

$$T = .313 \times B \pm .005 \times B$$
$$S = .130 \times B \pm .010 \times B$$
$$W = 1.500 \times B \pm .010 \times B$$

$$B = \text{SPECIMEN DIAMETER}$$

25.4 mm (1 in):   B = 25.4 ± .01 mm (1.000 ± .004 in)
19.05 mm (3/4 in): B = 19.05 ± .007 mm (.750 ± .003 in)
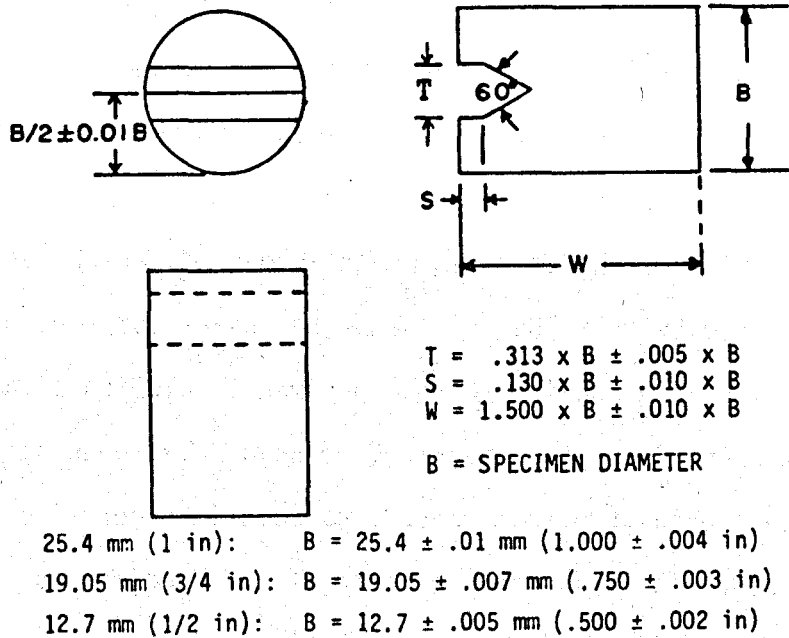12.7 mm (1/2 in):   B = 12.7 ± .005 mm (.500 ± .002 in)

Figure 11. Short-rod specimen geometry.

tested. Diameters as small as 1.0 $(K_{Ic}/\sigma_{ys})^2$ (where K_{Ic} is the toughness and σ_{ys} is the yield strength of the steel) can be tested by the short-rod technique whereas the thickness of the ASTM E399 compact toughness specimen must be at least 2.5 $(K_{Ic}/\sigma_{ys})^2$.[7]

Several loading devices have been developed for short-rod testing including a machine called a "fracjack", shown in Figure 12. The frac-jack is installed in a tensile testing machine as illustrated in Figure 13. The specimen is placed over the grips on the fracjack (see Figure 14) and a copper chamber with cartridge heaters is installed over the steel specimen as shown in Figure 15. A thermocouple, placed in the cheveron-shaped slot, is connected to a controller which supplies power to the heater cartridges. For specimens tested at elevated temperatures, the chamber was installed, brought to the desired temperature then held five minutes before applying a load. The equipment used to test 50.8 mm dia-meter short-rod samples is shown in Figure 16. 25.4 mm diameter specimens were tested in a Fractometer[11] which employs smaller grips and a smaller heater to perform the test in the same manner. Actuating the test machine (see Figure 16) causes the grips to force the specimen mouth open. The fracjack rotates the grips as the specimen mouth is opened, which results in lines of constant load between the grips and the inside surfaces of the specimen mouth. The load applied to the specimen is plotted as a function of the mouth opening of the specimen, or Load Point Opening (LPO), which generates a load versus LPO test record, as seen in Figure 17. The initial loading slope is linear as the mouth of the specimen is elastically opened by the grips. Eventually, the load-LPO trace deviates

18
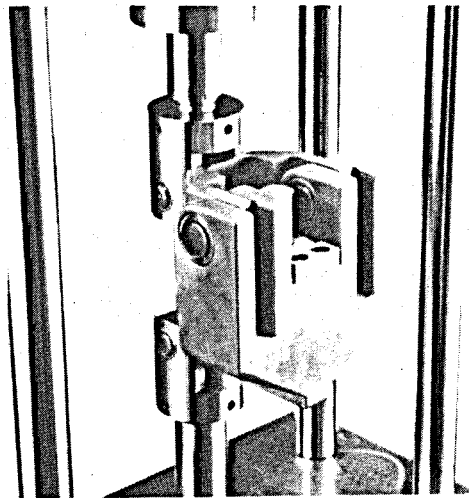
Figure 12. Fracjack loading device with specimen installed over grips.
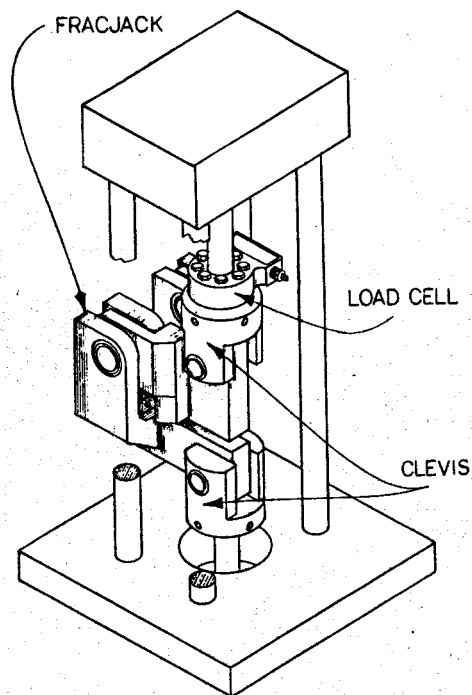
Figure 13. Fracjack located in tensile testing machine.
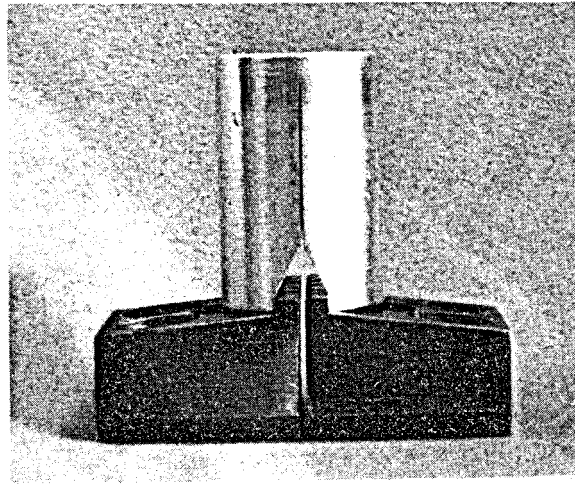
Figure 14. Installation of a specimen on the fracjack grips. The short-rod sample is shown installed on grips which have been re-moved from the fracjack.
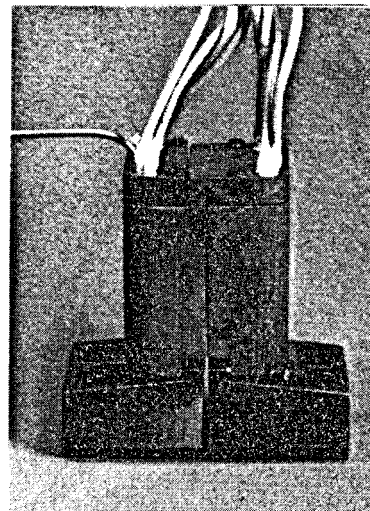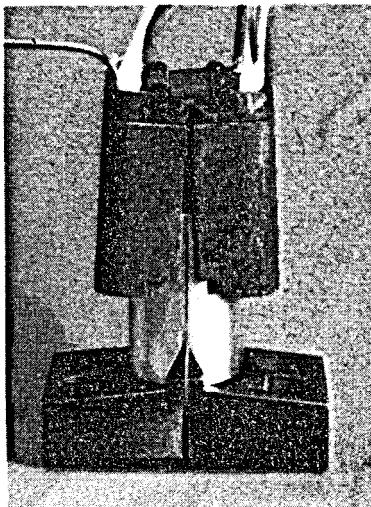
Figure 15. Installation of the temperature control chamber over a short-rod.
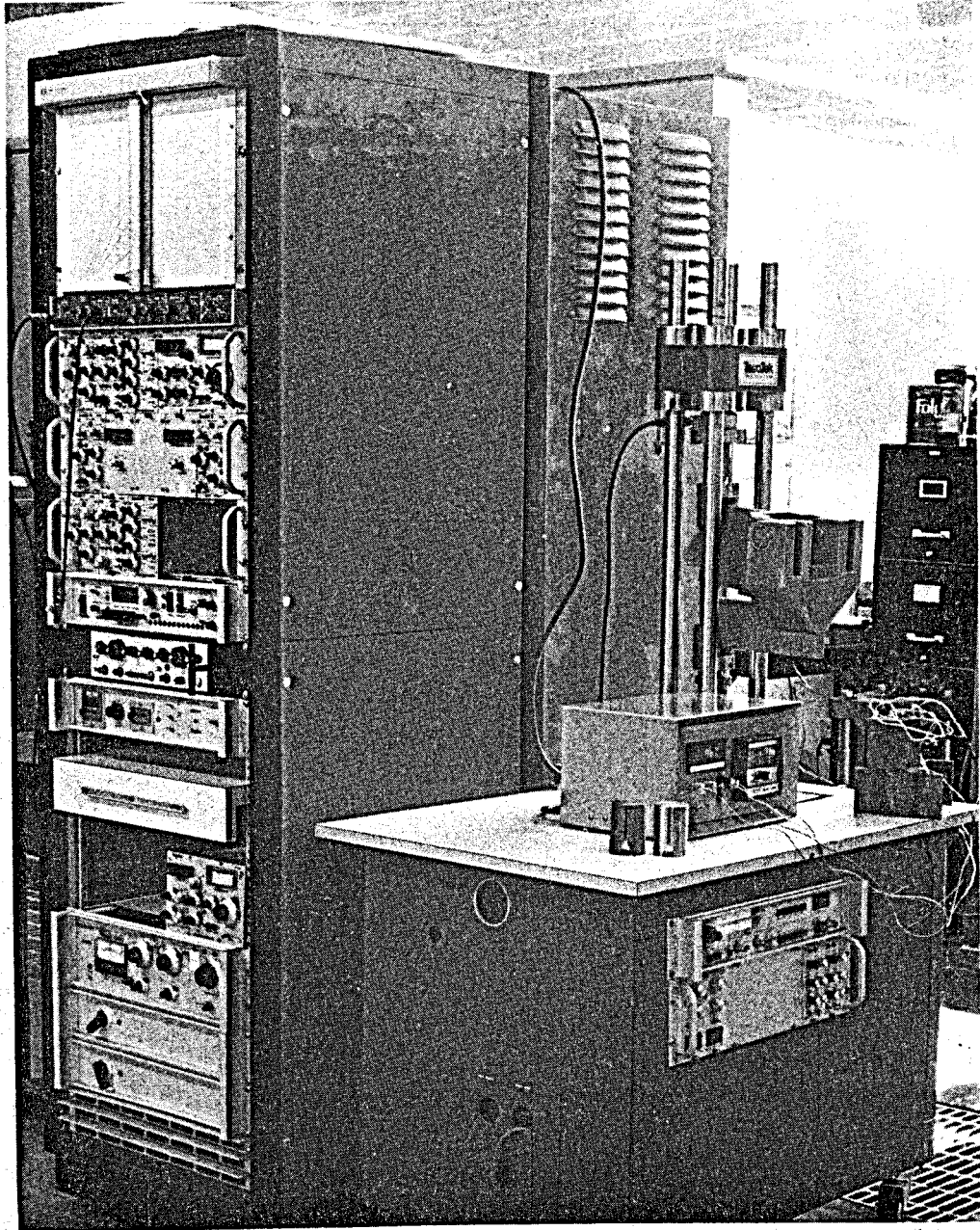
Figure 16. Tensile testing machine, control panel and temperature con-
troller used for short-rod fracture toughness and fatigue
measurements.

21

LOAD

LOAD POINT OPENING
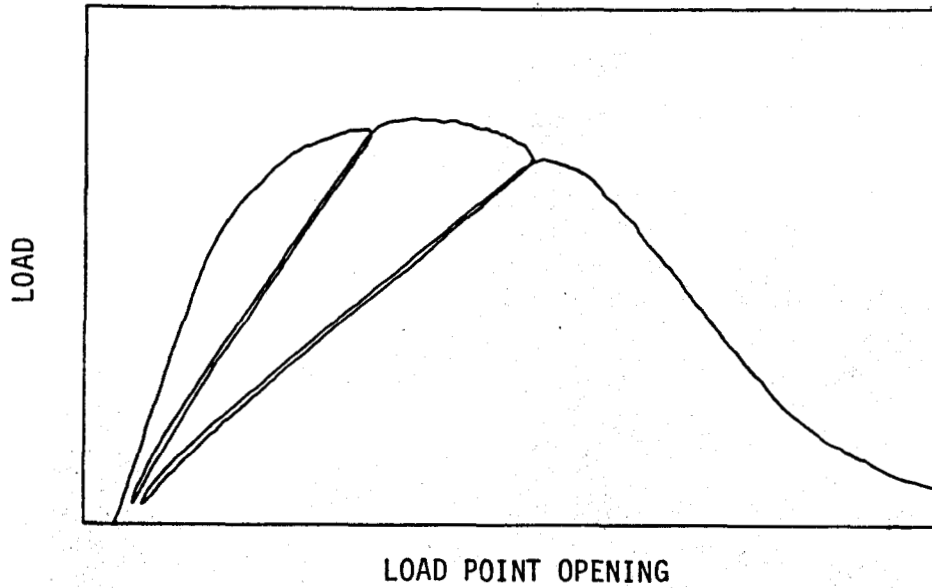
Figure 17. Load versus LPO test record for a steel sample with minimal plasticity.

from linearity indicating that a crack has initiated at the point of the V. Increasing the load causes stable crack growth which constantly widens the crack front. The fracture toughness measurement is made in the region of the maximum load after the crack has grown into the central region of the specimen. The load is released and reapplied several times during the test (two unloading-reloading sequences are seen in the test record in Figure 17) to determine and correct for residual stresses and plasticity. In several of the steel specimens tested, the plastic zone associated with the crack tip was appreciable, causing the stretched material within the zone to prop the mouth slightly open after the external load was released. The degree of plasticity is easily determined from the test record and the effect of the plastic zone on the indicated toughness is known[7].

Macroscopic residual stresses also affect the measurement of the fracture toughness by causing the test crack to be in a state of tension or compression before the application of any external load. The effects of residual stresses in short-rod specimens can be detected and compensated for in much the same way that the specimen plasticity is measured[12].

In some cases, the phenomenon of crack closure[13] causes the unloading paths to become nonlinear after most of the unloading has occurred. Crack closure is caused by material on the crack surfaces which has been pulled out or disturbed during fracture to partially fill the space between the two fractured surfaces. The steepening of the unloading paths resulting from the early closure of the crack does not affect the fracture toughness measurement but does limit the range in which loads can be applied during fatigue testing.

Several of the steel specimens tested exhibited "crack-jump behavior" rather than the smooth crack growth described above. These specimens had load-displacement test records which consisted of a few very rapid jumps in crack position. Each crack jump was accompanied by an audible "pop" and a decrease in the applied loading force. Between the jumps, as loading continued, the crack was nearly stationary until the load was increased to a level which precipitated the next jump. Although specimens displaying crack-jump behavior do not allow for unloading-reloading cycles so that the effects of plasticity or residual stress can be included in the determination of fracture toughness, they do provide insight into the mode of fracture, as discussed later (see Results and Discussion Section).

The loading sequence of the short-rod fracture toughness test was completed in less than one minute for specimens exhibiting either smooth crack growth of crack-jump behavior.

Fatigue Crack Resistance Measurements

Identical specimens to those used in static fracture toughness measurements were used to determine the fatigue behavior of the steels. Fatigue tests were performed at room temperature for AISI 4820, 8620 and 9315, and at 300°C for CBS 600, CBS 1000M, EX-00053 and Vasco X-2M. 50.8 mm diameter cylinders were used for all steels except 9315 in which 25.4 mm diameter specimens were tested. All measurements were made in air and although the humidity was not monitored, it was relatively constant near 25 percent.

A Textronix 531A oscilloscope was used to monitor the load-displacement behavior for all fatigue testing and a Polaroid camera made permanent record of the tests. The sample was placed in the fracjack loading device and the appropriate temperature was obtained and monitored throughout the test. The specimen was initially loaded and the slope of the load-displacement line recorded. The specimen was then further loaded to initiate a crack before fatigue cycling began. All samples were cycled at 5 Hz with the specimens being loaded and unloaded in tension. The initial minimum and maximum loads were not identical for all samples since crack closure effects varied and it was necessary to avoid crack closure in all instances.

After the crack was initiated, the specimen was cycled between two constant loads and the average difference between the loads was used to determine an average ΔK in an identical manner to that used in static fracture

toughness tests[7]. Crack advance was measured using previously determined compliance calibrations[9,10] by correlating the change in the slope of the load-displacement curves from the oscilloscope with the initial crack length and loading slope determined at the beginning of the test. The maximum load was increased periodically throughout the test, thereby increasing ΔK and allowing several ΔK values to be measured from one sample. The loading-unloading slope, and hence the change in compliance, was recorded each time just before the load was increased and the number of cycles was also recorded from the test machine. A typical test consisted of approximately 100,000 cycles and five to ten ΔK levels. A plot of the rate of crack growth as a function of the change in toughness was made by applying the Paris power law[14]:

$$\frac{da}{dN} = C(\Delta K)^m \qquad (1)$$

where da/dN is the fatigue crack growth rate, ΔK is the cyclic stress intensity ($\Delta K = K_{max} - K_{min}$) and C and m are material constants dependent on frequency, temperature, environment and stress ratio. To eliminate the effect of changing stress ratio on the data[15], the following relationship was used[16]:

$$\frac{da}{dN} = \frac{C(\Delta K)^m}{\sqrt{1 - R}} \qquad (2)$$

where R is the stress ratio ($R = K_{min}/K_{max}$) and all other symbols are the same as in Equation 1. The fatigue crack growth at a specific ΔK was determined by dividing the change in crack length (Δa) by the number of cycles (ΔN) recorded during the constant ΔK period of the test.

RESULTS AND DISCUSSION

Steel Characterization

Only limited characterization of the steels has been performed at this time. Radian Corporation, with support from DOE/DGE Chicago Operations Program, analyzed each of the steels in the test program, with results displayed in Table 5. The chemical analyses performed by the Timken Company for CBS 600, CBS 1000M and 9315 (see Table 4) agree well with the Radian results except for the nickel content of 9315. The compositional differences between the two heats of CBS 600 and CBS 1000M should be noted. It should also be observed that, as expected, EX-00053 had the lowest carbon content of the steels tested and that 9315 had a considerably lower carbon content than either 4820 or 8620.

Radian Corporation also measured the hardness (Rockwell C) of the fractured steel specimens. Decarburization was noted on the surface of several of the samples but this had no effect on toughness or fatigue measurements because of the configuration of the test specimens. Hardness measurements were made at approximately every 1.6 mm from the surface to the center of each specimen, with results shown in Table 6. The bracketed hardness value best describes the hardness in the center of the specimen. The Timken Company measured the surface hardness of test cylinders after heat treatment and found values of 41.5 R_c for 25.4 mm and 38 R_c for 50.8 mm specimens. The hardness at the center of CBS 600 specimens, as determined by Radian, was R_c 39.0 for 25.4 mm and R_c 38.0 for 50.8 mm specimens. Timken measured a surface hardness of 37 R_c for

TABLE 5

Chemical Analysis (Percent by Weight)

Steel Type	C	Mn	P	S	Si	Cr	Ni	Mo	V	W	Cu
4820	0.18	0.63	0.008	0.013	0.29	--	3.31	0.22	--	--	--
8620	0.20	0.75	0.007	0.017	0.19	0.49	0.46	0.18	--	--	--
9315	0.12	0.58	0.009	0.006	0.31	1.31	3.44	0.17	--	--	--
CBS 600	0.20	0.71	--	--	1.21	1.38	--	1.02	--	--	--
CBS 600*	0.19	0.63	0.008	0.006	1.06	1.58	--	1.04	--	--	--
CBS 1000M	0.14	0.57	--	--	0.50	0.80	3.20	4.13	0.32	--	--
CBS 1000M*	0.15	0.62	0.011	0.005	0.51	1.07	3.32	4.40	0.34	--	--
EX-00053	0.093	0.30	--	--	0.99	0.81	2.05	3.15	0.09	--	1.81
X-2M	0.13	0.21	--	--	0.99	4.49	0.05	1.28	0.36	0.72	--

* Separate Heat (used for 25.4 mm cylinders).

TABLE 6

Characterization of Steels

Steel Type	Heat Treatment[4]	Core Hardness (R_c)	Grain Size (McQuaid Ehn)	Yield Strength (2% Offset)[3]		Tensile Strength[3]	
				MPa	KSI	MPa	KSI
4820[2]	A	37.0-42.5 (38.0)	8-9	869	126	1,172	170
8620[2]	B	20.5-28.5 (22.0)	7-8	827	120	1,151	167
9315[1]	C	34.0-39.5 (35.5)	7	848	123	1,096	159
CBS 600[1]	D	39.0-41.0 (39.0)	6	1,262	183	1,172	170
CBS 600[2]	D	37.5-39.0 (38.0)	6	1,262	183	1,172	170
CBS 1000M[1]	I	36.5-39.5 (38.5)	6	1,124	163	1,323	192
CBS 1000M[2]	G	37.0-40.0 (38.5)	5-6	1,124	163	1,323	192
EX-00053[2]	L	31.5-35.0 (32.0)	Finer than 10	965	140	1,159	168
X-2M[2]	M	37.5-40.0 (38.5)	8-9	1,034	150	1,379	200

1 - 25.4 mm diameter specimen

2 - 50.8 mm diameter specimen

3 - Manufacturer's data

4 - See Appendix A for explanation of heat treatment code.

50.8 mm CBS 1000M specimens and 43.0 R_c for the same heat treatment of
25.4 mm specimens. Radian measurements resulted in essentially identical
hardness values for the two heats.

McQuaid-Ehn grain size (ASTM E112 A.3.2.1.1-78) as determined by
Radian Corporation is listed in Table 6. This procedure is based on
determining the austenite grain size after carburization and does not
necessarily produce a valid measure of the prior austenite grain size in
specimens in the condition in which they were tested. The Timken Company
etched the 25.4 mm diameter CBS 1000M specimens in Villela's etch and
measured a prior austenite grain size of 10 to 11, considerably finer
than determined by Radian, and a structure of tempered martensite with
M_6C carbides. The 25.4 mm diameter CBS 600 specimen, quenched from 835°C
(treatment D), when etched in 4 percent Nital, displayed a grain size of
7 and a duplex microstructure consisting of tempered martensite with 40
percent lamellar ferrite. When the same steel was austenitized at 870°C
(treatment F), the microstructure was completely tempered martensite and
the grain size was 7 to 8. Etching of the other steels is underway to
determine both ASTM grain size and microstructure. The only conclusion
that can be derived from the McQuaid-Ehn grain size measurements is that
the Carpenter EX-00053 steel has a very fine grain size.

Radian determined that the microstructures of 9315, EX-00053 and
X-2M, after the treatments listed in Appendix A, consist entirely of
tempered martensite. Continuous cooling transformation diagrams predict
a microstructure consisting of nearly 100 percent bainite with a trace of
martensite for a 50.8 mm diameter 4820 rod water quenched from 780°C and

29

an identical cylinder made of 8620 should have a microstructure at the center consisting of about 50 percent ferrite, 45 percent bainite and 5 percent martensite after water quenching from 830°C. It is apparent that the microstructures of 4820 and 8620 will vary over the width of the crack in a short-rod specimen and that characterization of the grain size and microstructure in these steels is important. Tabulation of the yield strength and tensile strength of steels, based on manufacturer's data in Table 6, indicates that each of the candidate steels have higher strengths than the conventional steels presently in use.

Scanning electron microscopy (SEM) of the fractured surfaces was performed by Radian Corporation. Selected micrographs are displayed in Appendix B (Figures B1 through B18). The SEM micrographs seen in Figures B19 through B32 represent comparison fracture surfaces from static and fatigue test samples and were taken by Terra Tek at the University of Utah. The fracture mode was transgranular for all specimens. The degree of ductility estimated by Radian from their SEM micrographs is listed in Table 7. Also included in Table 7 is the observed crack behavior from load-displacement test records. It is interesting to note that the brittle-to-ductile transitions noted in CBS 1000M, EX-00053 and X-2M between room temperature and 200°C correlate well with the observed crack behavior from the test records. There is, however, no information from the SEM micrographs to explain the crack jump behavior observed in 8620, 9315, CBS 600 and CBS 1000M at high temperatures.

TABLE 7

Fracture Mode Based on SEM Micrographs

Steel Type	Fracture Temperature (°C)	Degree of Ductility	Crack Behavior
4820	RT†	A	S
	100	A	S
	200	A	S
	300	A	S
8620	RT	C	S
	100	B	S
	200	A	S
	300	A	S-J
9315	RT	A	S
	100	A	S
	200	A	S
	300	A	S-J
CBS 600	RT	A	S
	100	A	S
	200	A	S
	300	A	S
	400	A	J
CBS 1000M	RT	D	J
	100	A	S
	200	A	S
	300	A	S
	400	A	J
EX-00053	RT	B	J
	100	A	S
	200	A	S
	300	A	S
	400	A	S
X-2M	RT	E	J
	100	E	J
	200	B	S
	300	A	S
	400	A	S

† RT - Room Temperature

A - Ductile, microvoid coalescence
B - Mixed Mode, less than 25% brittle cleavage
C - Mixed Mode, 25-75% brittle cleavage
D - Mixed Mode, greater than 75% brittle cleavage
E - Brittle Cleavage

S - Smooth Crack Growth
J - Crack Jump Behavior
S-J- Borderline Between Smooth and Crack Jump

31

Fracture Toughness

The experimental data from static fracture toughness tests are tabulated in Appendix A along with heat treatments. A description and interpretation of the data follow.

AISI 4820: The toughness of 4820 (heat treatment A) as a function of temperature is shown in Figure 18. The steel was tested with slots and grip grooves machined before heat treating, as well as machining performed after heat treating, with no observed difference in the fracture toughness. The fracture toughness declines steadily with temperature to 200°C and then increases slightly between 200 and 300°C. SEM micrographs revealed dimpled rupture indicative of ductile fracture at all temperatures. Although there is no obvious reason for the decrease in toughness with temperature, the increase above 200°C may be due to microstructural changes occuring during the test, because the tempering temperature was only 230°C[17]. The important observation is that the toughness at 200°C is only half the value of the fracture toughness at room temperature.

AISI 8620: The low hardenability of 8620 (heat treatment B), relative to other steels tested, caused differences in the fracture toughness depending on whether the cylinders were slotted before or after heat treating (see Figure 19). The specimens heat treated after slotting showed considerable scatter between tests due to residual stresses arising from quenching and phase transformation. The specimens quenched without slots displayed consistently higher toughness at room temperature and 300°C then their slotted counterparts, but no difference was observed at
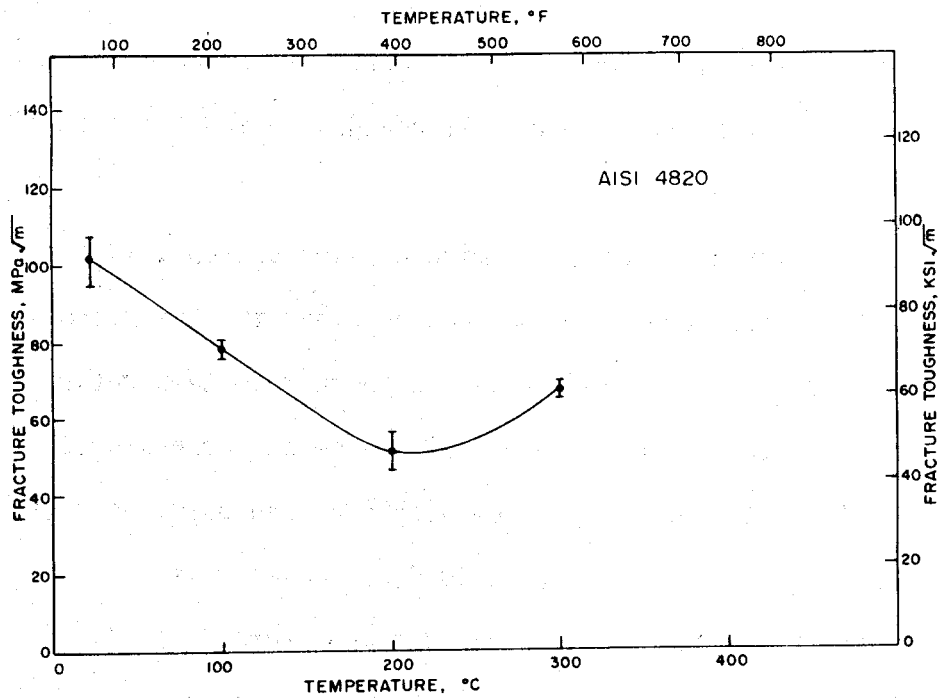
Figure 18. Fracture toughness as a function of temperature for 4820 (heat treatment A).
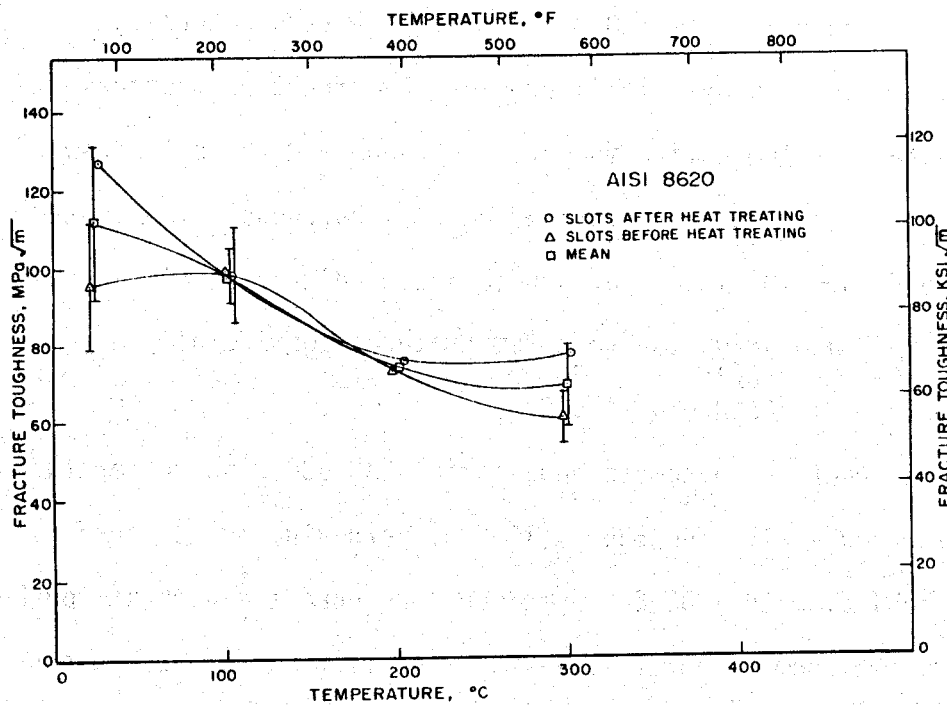

Figure 19. Effect of temperature on the toughness of 8620 (heat treatment B).

33

100°C and 200°C. As for 4820, the 300°C test temperature exceeded the 230°C tempering temperature, so microstructural changes during the test were inevitable.

The obvious trend, regardless of the timing of slot cutting, is a drop in toughness with temperature, despite the fact that the SEM micrographs indicate some degree of brittle cleavage at both room temperature and 100°C and ductile fracture by microvoid coalescence at temperatures of 200°C and 300°C. The most serious problem with 4820 and 8620, however, is the drop in hardness between ambient and 200°C, since wear is greatly accelerated in these steels by increased temperature.

AISI 9315: The 9315 steel (heat treatment C), with its entirely martensitic structure as well as high nickel and low carbon contents, displayed the best toughness of any of the conventional steels tested. The toughness decreased only from 120.7 MPa√m at room temperature to 88.0 MPa√m at 300°C, as displayed in Figure 20. The fracture toughness of 9315 is adequate over the entire temperature range and the only drawback to this steel is its poor wear resistance (low hardness) at elevated temperatures (see Figure 10) in comparison to the candidate steels in the program. As for 8620 and 4820, the test temperatures considerably exceeded the tempering temperature of 175°C.

CBS 600: The fracture toughness behavior of CBS 600 with temperature is illustrated in Figure 21. The 835°C (1535°F) hardening temperature of the 50.8 mm (2 inch) diameter CBS 600 specimens produced the highest toughness (154.1 MPa√m) in room temperature tests. The microstructure had considerable ferrite mixed with the martensite. When the same heat treatment
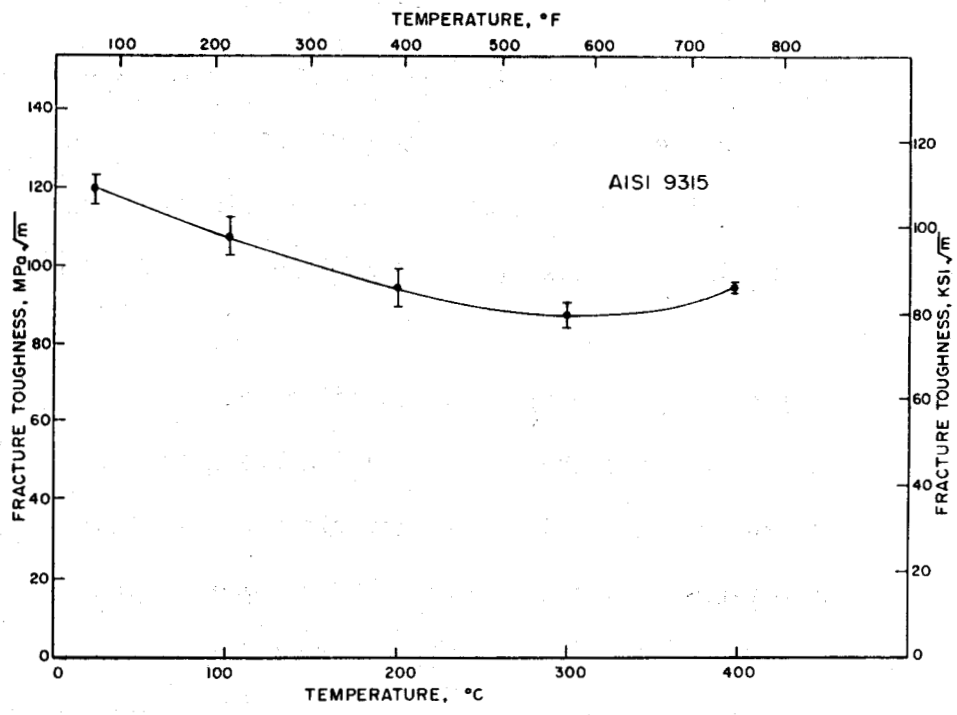
Figure 20. Fracture toughness of 9315 as a function of temperature (heat treatment C).
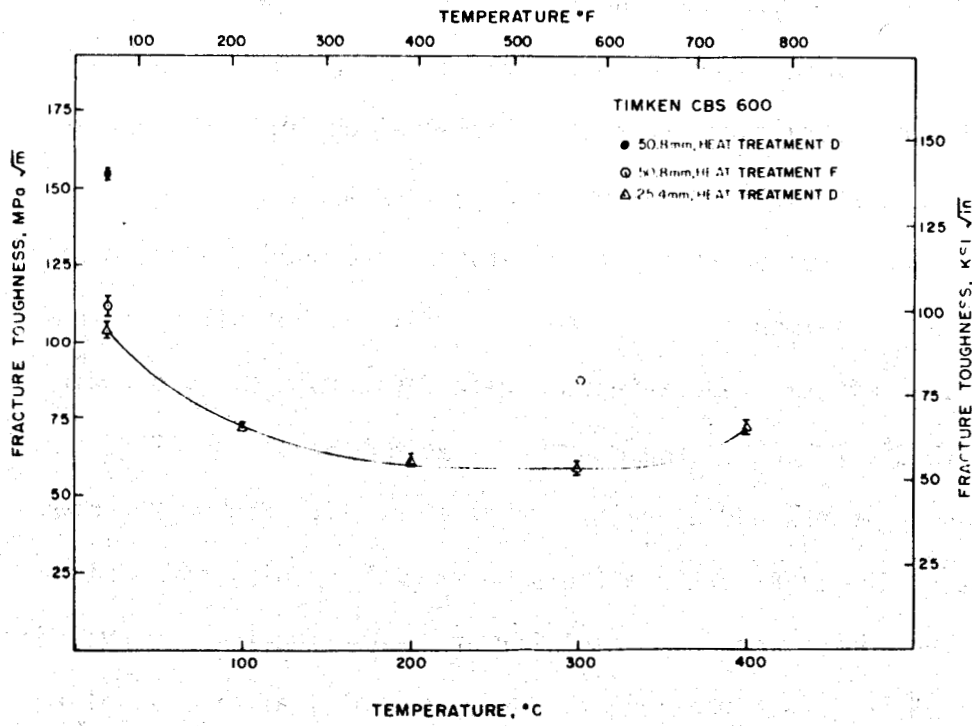

Figure 21. Effect of temperature on the toughness of CBS 600.

35

was applied to 25.4 mm diameter specimens, 40 percent lamellar ferrite was observed. The 25.4 mm specimens were significantly less tough at room temperature than were the 50.8 mm specimens (see Appendix A). The toughness of the 25.4 mm specimen drops sharply from 103.5 to 61.5 MPa√m between room temperature and 200°C.

The 870°C (1600°F) hardening temperature produced an entirely martensitic microstructure with about the same austenite grain size as the 835°C "austenitizing" temperature. It is interesting to note that the 100 percent tempered martensite microstructure had a lower toughness at room temperature (111.4 MPa√m) than the ferrite-martensite cylinders of the same size. The room temperature hardness was 42.5 R_c for the martensitic structure and 38.0 R_c for the martensite-ferrite microstructure indicating a trade-off in hardness and toughness. A cylinder hardened at 870°C had a toughness of 86.9 MPa√m at 300°C, perhaps indicating that a totally martensitic structure may retain toughness better with increasing temperature than microstructures containing ferrite.

CBS 1000M: Three austenitizing temperatures were used in determining the effects of heat treatments on K_{Ic} (see Appendix A), but all specimens had microstructures of tempered martensite with M_6C carbides. The grain size after the 1090°C (2000°F) treatment was 7 to 8 whereas the 955°C (1750°F) treated cylinders had a grain size of 10 to 11. Figure 22 shows that, as expected, the finer-grained (hexagon shaped symbols) had a higher toughness than the coarser-grained steel (triangles). The 25.4 mm cylinders austenitized at 955°C (heat treatment I, square symbols) after a simpler heat treatment than its 50.8 mm counterpart (heat treatment G, hexagons)
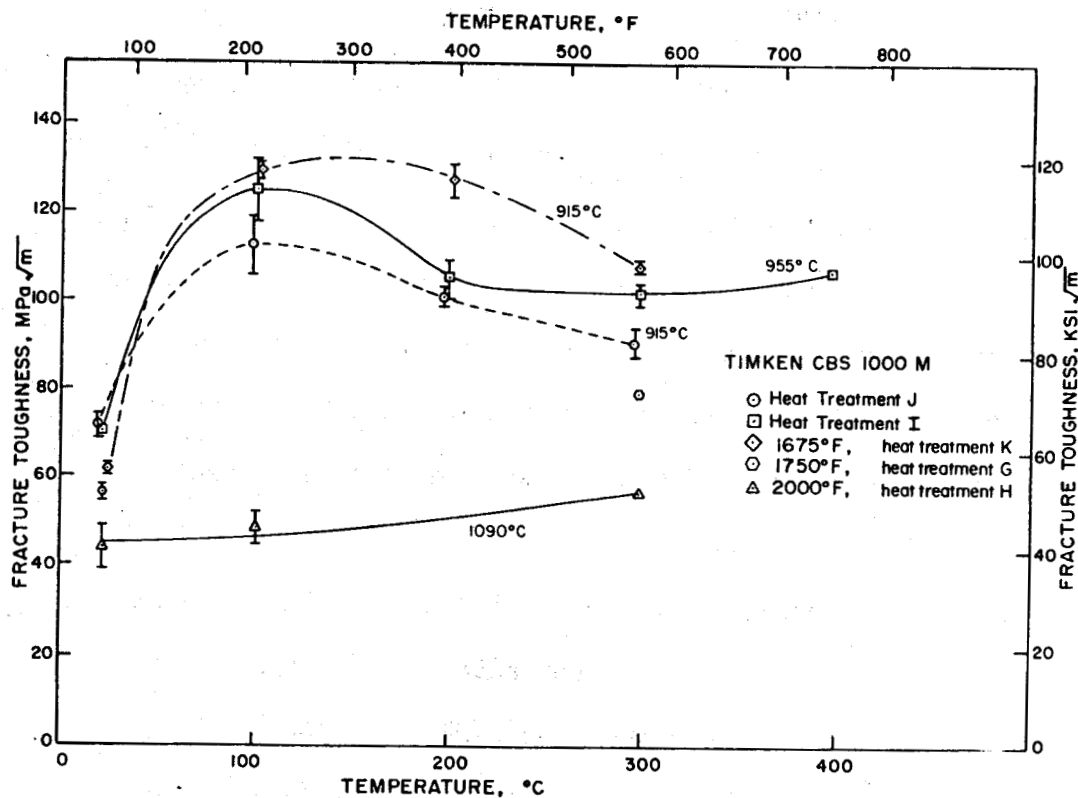
Figure 22. Temperature dependence of toughness for CBS 1000M.

had a higher hardness (43 R_c versus 37 R_c) as well as increased tough-
ness (80.0 MPa√m̄ versus 57.1 MPa√m̄). As previously discussed, the hard-
ness of this steel is in question since Radian measured a hardness of
39.5-38.5 R_c at the center of both size cylinders. It is obvious, how-
ever, that hardness is not always sacrificed when improved toughness is
obtained.

The most intriguing result of the CBS 1000M tests was the large in-
crease in toughness between room temperature and 100°C. This increase
in toughness correlates well with the brittle-to-ductile fracture transi-
tion of this steel as seen in micrographs B9-B11 (Appendix B). All CBS
1000M specimens had excellent toughness retention over the entire tempera-
ture range.

37

Except for austenitizing at 1090°C, all the heat treatments given

CBS 1000M produced adequate toughness for any drilling application above

room temperature. The low ambient temperature toughness, as compared to

4820, 8620 and 9315, would limit the use of this steel in the cold environ-

ments sometimes encountered in normal rock drilling. As can be seen

from Figure 10, the CBS 1000M has the best wear resistance of any steel

in the test program. However, its high cost and elaborate heat treatment

militate against its wide-spread use.

EX-00053: The room temperature toughness (103.6 MPa$\sqrt{m}$) of EX-00053,

heat treatment L, is comparable to that of conventional steels but the

increase in toughness at 100°C is phenomenal (265 MPa$\sqrt{m}$). The steel

appears to be going through a brittle-to-ductile transition (see Figures

B13 and B14, Appendix B) in this temperature range (see Figure 23). Even

in 50.8 mm diameter specimens and employing the short-rod technique, the

toughness is difficult to measure because of the large plastic zone in

the test cylinders. The EX-00053 steel should be an excellent candidate

for any application requiring exceptional toughness at elevated tempera-

tures. Further studies are essential to determine the cause of the rapid

increase in toughness of this steel in a small temperature interval.

X-2M: The X-2M steel displayed the most consistent toughness behavior

as a function of temperature of any steel tested (see Figure 24). Un-

fortunately, the toughness of this steel is also the lowest of any tested

and although it is comparable to 4820 and 8620 in the 200 to 300°C range,

the low room temperature toughness does not make this steel a promising

candidate for geothermal rock bits since the bits must be able to withstand
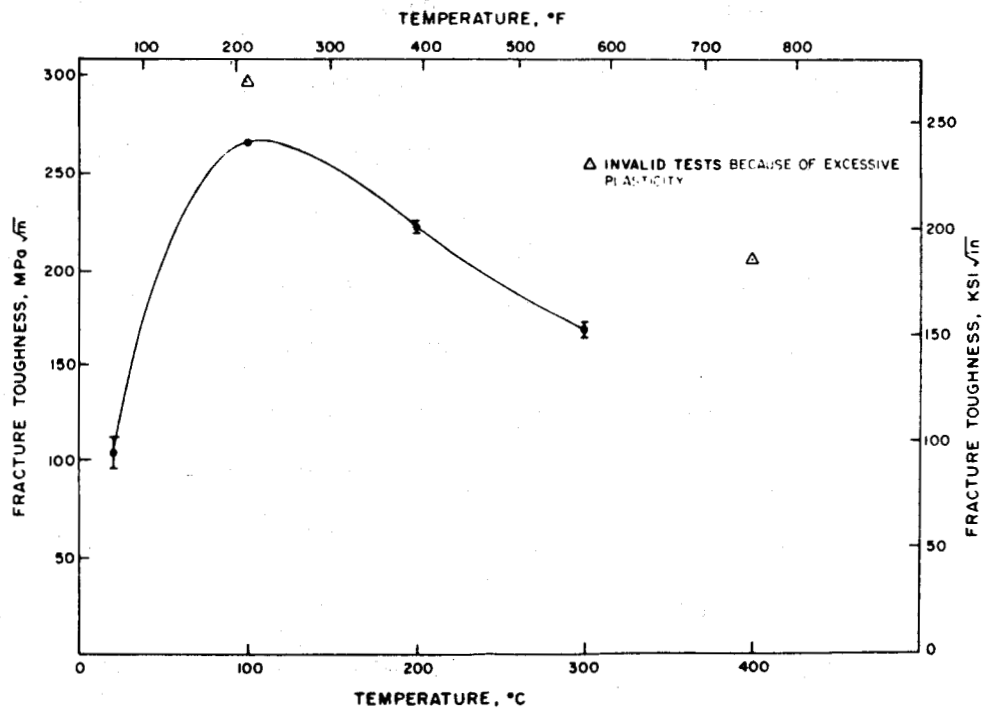
Figure 23. Effect of test temperature on fracture toughness of EX-00053 (heat treatment L).
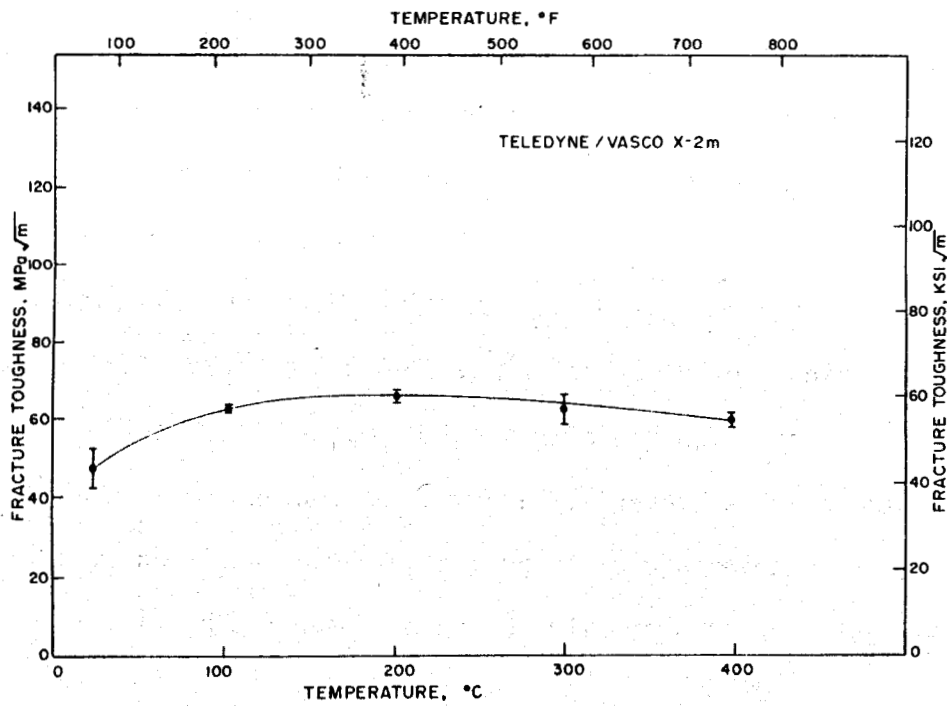

Figure 24. Effect of temperature on the toughness of X-2M (heat treatment M).

impact during fabrication and shipping. The main problem with this steel, however, is the high austenitizing temperature (1120°C) which calls for furnace equipment not generally used by bit manufacturers.

One interesting result of the X-2M tests is the excellent correlation between the crack behavior observed on the test record and the brittle-to-ductile transition temperature (see Table 7). The SEM micrographs (see Figures B15-B18) reveal that the steel changes from very brittle cleavage to ductile fracture between 100°C and 200°C, accompanied by a change from crack-jump behavior to smooth crack growth. Surprisingly, there was not corresponding increase in toughness between 100°C and 200°C.

The toughness of the steels tested is compared in Figure 25. It is very apparent that EX-00053 has superior toughness at elevated temperatures and that CBS 1000M is the only other steel which has K_{Ic} values equal or superior to 9315. The other obvious trend is that steels with tempered martensite structures (X-2M, 9315, CBS 1000M, EX-00053) have much better toughness retention with increasing temperature than steels containing ferrite or bainite (4820, 8620 and CBS 600). These latter steels drop rapidly in toughness with increasing temperature. Although all of the steels, with the possible exception of X-2M, may be capable of resisting fracture during geothermal drilling, EX-00053 and CBS 1000M appear to be the only steels capable of resisting impact fracture if reamers and bits made of these materials are used at conventional penetration rates. The obvious advantage of using a highly wear-resistant steel would be to drill faster and longer with the same or reduced bearing wear.
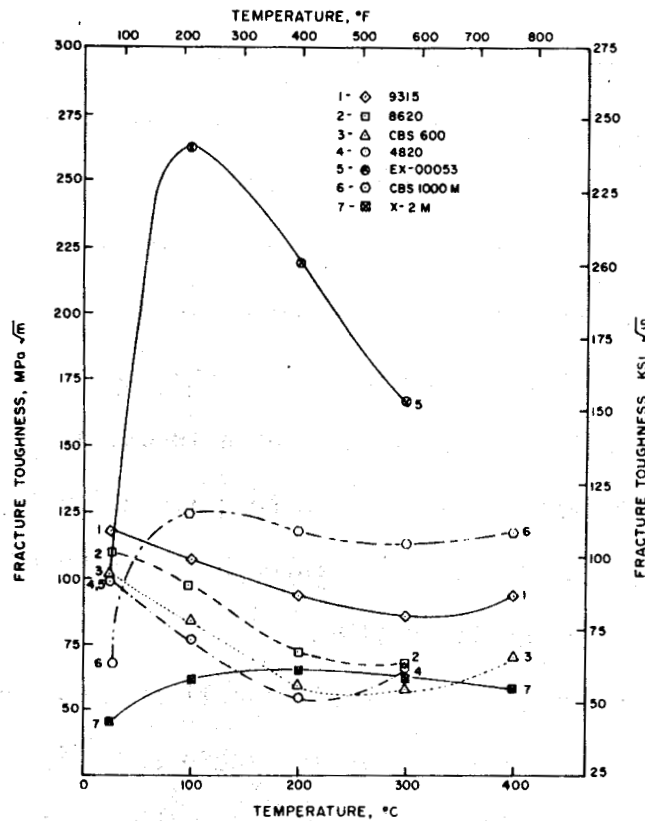
Figure 25.   Toughness comparison of conventional and high
              wear resistant steels.

Fatigue Crack Resistance Measurements

Extensive data[18] on fatigue crack growth behavior in metallic systems
have been generated. These studies have proven the validity of the Paris
power law in the region where stable crack growth occurs[16]. The approach
is useful because a knowledge of fracture toughness and fatigue properties
allows an estimate to be made of the maximum allowable initial flaw size
if the operating stress level is known. Alternatively, it is possible to
estimate a maximum allowable stress for a given flaw which will not allow
it to grow to critical dimensions during the intended life of the com-
ponent[16]. Although fatigue data are not presently used to predict bit
failure, it was believed that wear-resistant steels should have fatigue

41

behavior at high temperatures similar to that of conventional bit steels at room temperature. This maybe an over-simplification since conventional rock bits certainly operate at elevated temperatures.

It was expected that m values from the Paris power law[16] would be in the range of two to four for all steels tested and that the slopes would simply be shifted to higher or lower crack propagation rates if a log-log plot of crack propagation rate was made as a function of stress intensity factor. The test results, however, were quite different, as can be seen in Table 8, and in Figures 26 through 33. A brief discussion of the individual test results follows.

AISI 4820: Although no data were found in the literature for crack propagation rates in 4820, the results shown in Figure 26 indicating an m value of 3.05 are reasonable. The line indicating the fit of the data is extended beyond the actual data points and it should be noted that the curve will bend down at low propagation rates and curve up at higher rates due to crack initiation and unstable crack growth, respectively. It is generally believed that the region between 0.1 and 10 μm/cycle is well within the stable region (often refered to as Region 2) of crack growth. 4820 showed little crack closure and as stated earlier, crack closure was avoided for all tests since cracks do not propagate when the crack has closed.

AISI 8620: An exceptionally high m value (11.38) was calculated from the test data and individual tests indicated an even higher m value of approximately 13.6. The first test was conducted with a specimen which was slotted before heat treating while the second test used a

TABLE 8

Fatigue Crack Resistance Results

Steel Type	Test Temperature (°C)	Test	$\frac{K_{max}}{(MPa\sqrt{m})}$	C [A]	M [B]	r [C]	Results Displayed in Figure
4820	RT [D]	1	62.6	4.14×10^{-10}	3.14	0.92	
	RT	2	60.8	5.90×10^{-10}	2.98	0.98	26
		Combined	62.6	4.87×10^{-10}	3.05	0.96	
8620	RT	1	70.1	1.67×10^{-25}	13.83	0.97	
	RT	2	80.7	7.91×10^{-26}	13.43	0.92	27
		Combined	80.7	2.36×10^{-22}	11.38	0.75	
9315	RT	1	73.4	1.23×10^{-7}	1.46	0.57	
	RT	2	78.4	8.73×10^{-3}	2.16	0.89	28
		Combined	78.4	1.71×10^{-9}	1.97	0.82	
CBS 600	300	1	65.4	2.24×10^{-17}	7.99	0.62	
	300	2	51.1	2.10×10^{-11}	4.29	1.00	29
		Combined	65.4	1.69×10^{-12}	4.92	0.40	
CBS 1000M	300	1	49.7	7.88×10^{-17}	8.24	0.96	
	300	2	64.0	4.22×10^{-10}	3.19	0.95	30
		Combined	64.0	1.22×10^{-7}	2.36	0.40	
EX-00053	300	1	94.6	1.08×10^{-14}	6.64	0.96	
	300	2	70.8	2.55×10^{-3}	1.01	0.11	31
		Combined	94.8	6.68×10^{-11}	4.68	0.59	
X-2M	300	1	46.5	1.80×10^{-13}	5.74	0.89	
	300	2	52.1	2.77×10^{-14}	6.40	0.98	32
		Combined	52.1	7.64×10^{-14}	6.04	0.93	

A - K_{max} = Maximum stress intensity factor during test   - r = Correlation coefficient squared

B - C,M = Constants as defined in Equation (2)   - RT = Room temperature
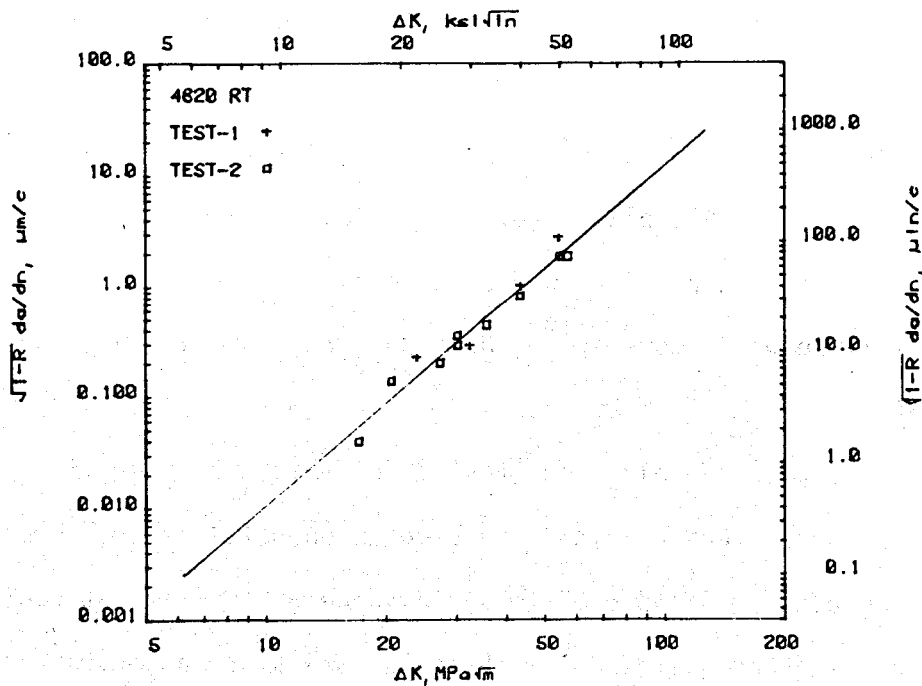
Figure 26. Crack growth rate as a function of stress intensity factor for AISI 4820.

43

cylinder which had been heat treated and then slotted. The similar results for both tests, as shown in Figure 27, indicate that residual stresses and microstructure were not the main reason for the anomalously high m value. The 8620 steel, however, displayed significant crack closure, such that a K_{min} of 50 MPa$\sqrt{m}$ and 62 MPa$\sqrt{m}$ were used for the two tests. The maximum stress intensity, 80.7 MPa$\sqrt{m}$, used in the second test approaches 70 percent of K_{Ic}. Although many investigators have produced evidence of accelerating rates of fatigue crack growth approaching final fracture, the separate contributions of ΔK and K_{max} have not been carefully examined[19]. It appears that both ΔK and K_{max} contribute towards the accelerating rates of crack propagation as the conditions for failure are approached. The high values of K_{min} and K_{max} required to reach the 20-40 MPa$\sqrt{m}$ ΔK range, due to crack closure, were apparently the cause of the steep slope of the log-log plot. It should be stressed that crack closure is not a peculiarity of the short-rod technique but is caused by plastic deformation or residual stresses within the specimens. The anomalous behavior is not entirely explained by crack closure constraints since high K_{max}/K_{Ic} ratios would normally cause crack growth rates above 10 μm/cycle if catastrophic failure were occuring[19]. No data were found in the literature for AISI 8620.

AISI 9315: 9315 was the only steel tested for which previous literature data could be found. Crack initiation studies on 9315[20] showed crack initiation occurring between 4 and 6 MPa$\sqrt{m}$ and a value of 10 MPa$\sqrt{m}$ at 0.01 μm/cycle. Figure 28 agrees quite well with these data since an extrapolation of the observed data for 9315 gives a ΔK of 5 MPa$\sqrt{m}$ at 0.01 μm/cycle. An m value near 2 is also consistent with what would be expected for room temperature measurements on this steel[16].
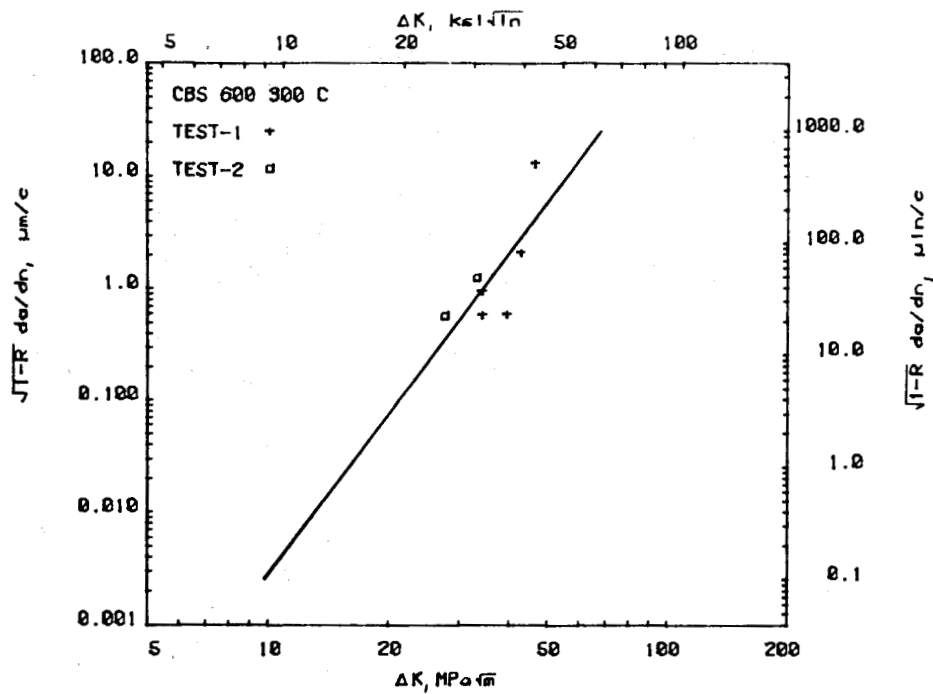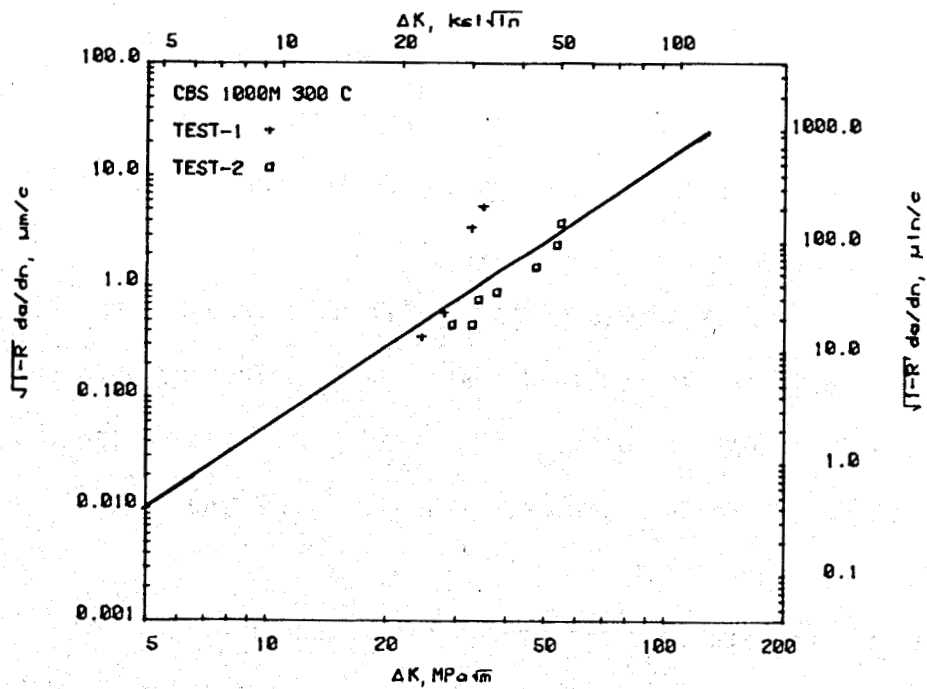
44
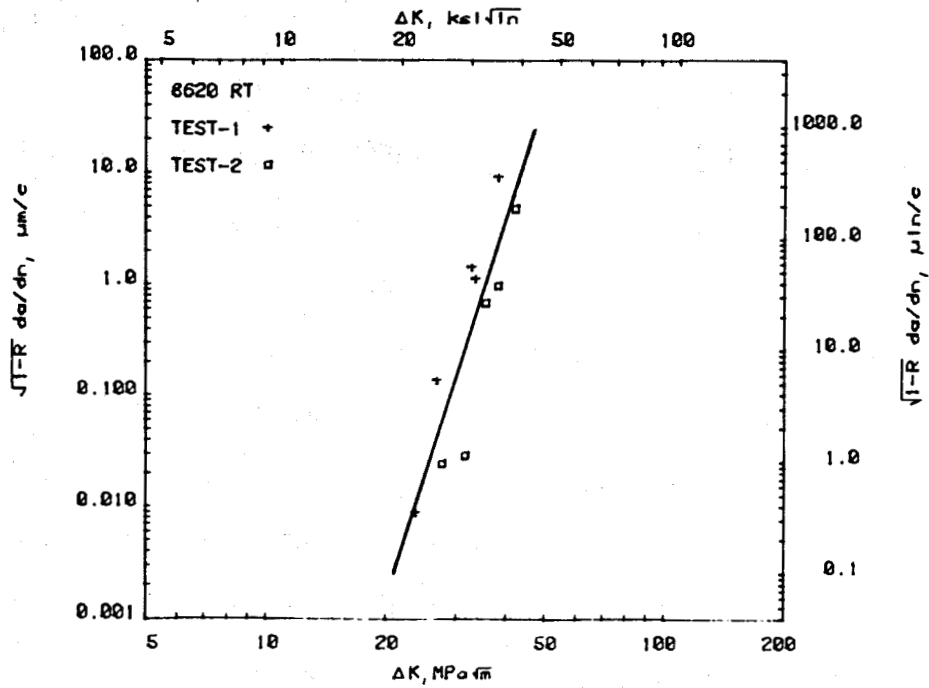
Figure 27.   Crack growth rate as a function of stress intensity
             factor for AISI 8620.
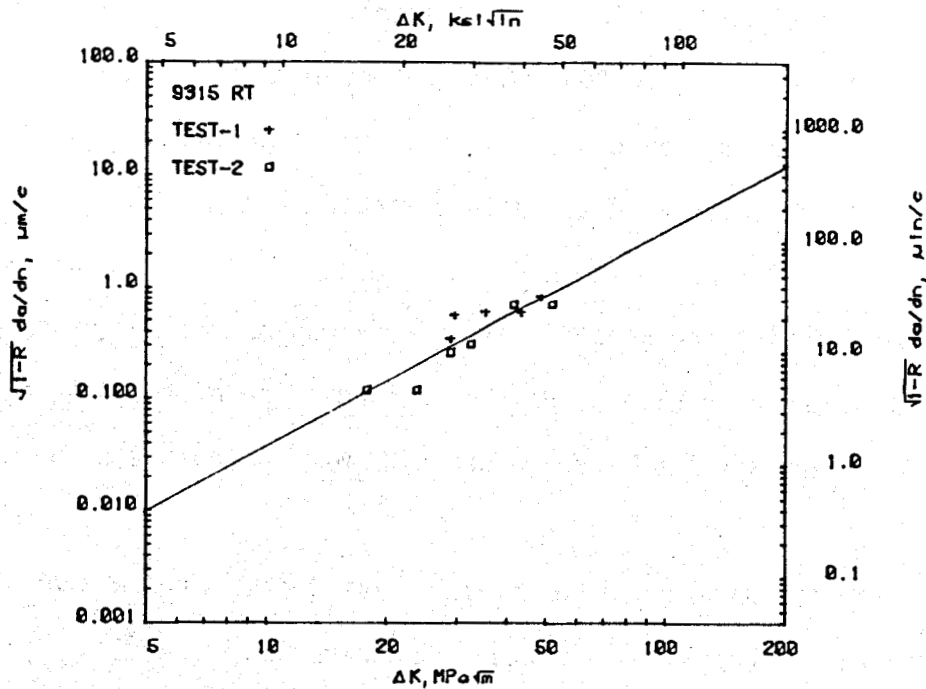
Figure 28.   Crack growth rate as a function of stress intensity
   factor for AISI 9315.

45

CBS 600: CBS 600 was tested at 300°C, as were CBS 1000M, EX-00053 and X-2M. Although it is widely known that temperature affects crack propagation rates[16] it is not clear whether temperature changes the m values or simply increases (or decreases) the crack propagation rate[19]. The tests of CBS 600 show a high degree of scatter in the data (see Figure 29) and the m value of 4.9 is therefore somewhat arbitary. The 50.8 mm diameter cylinders tested in fatigue were from the same heat treatment that produced the 154 MPa$\sqrt{m}$ room temperature static fracture toughness value. Although there were not enough 50.8 mm cylinders to test the static toughness at 300°C it is apparent that it drops rapidly, as evidenced by the 25.4 mm data and that the 65.4 MPa$\sqrt{m}$ K_{max} value is approaching K_{Ic} for the material. Crack closure was not a major problem with the lack of data at low crack growth rates. Longer testing at ΔK values near 20 MPa$\sqrt{m}$ would help to clarify the fatigue behavior of this steel.

CBS 1000M: The two tests on CBS 1000M gave different results as shown in Figure 30. The m value of 3.2 for test number two may be more valid than the combined value of 2.4. Both cylinders were austenitized at 955°C and the K_{Ic} for 79.5 MPa$\sqrt{m}$ in the static test at 300°C was approached by the K_{max} of 70.4 during the second test. There was only minor crack closure observed in these specimens and the extrapolation of the data below a ΔK of 20 MPa$\sqrt{m}$ is not advised since no crack growth was observed in this region.

EX-00053: No test data could be obtained for EX-00053 below a ΔK of 40 MPa$\sqrt{m}$, so the extrapolation of the line shown in Figure 31 below a ΔK of 40 MPa$\sqrt{m}$ is very arbitrary. The fact that all of the data

Figure 29.   Crack growth rate as a function of stress intensity
             factor for CBS 600.

Figure 30.   Crack growth rate as a function of stress intensity
             factor for CBS 1000M.
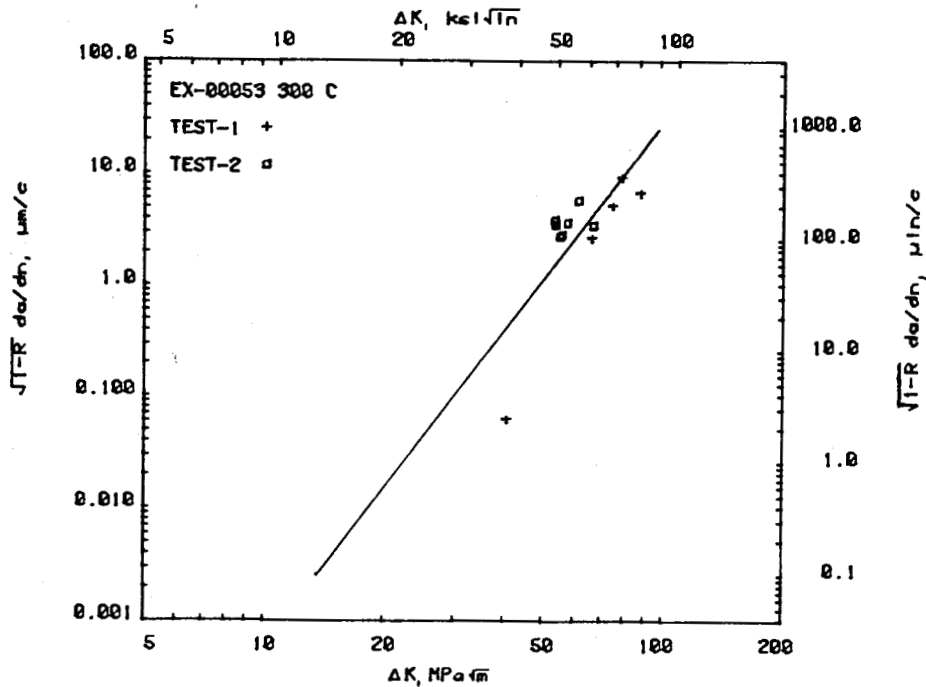
Figure 31.   Crack growth rate as a function of stress intensity
factor for EX-00053.

from the second test are clustered around 10 μm/cycle lowered the m value

from the 6.6 observed in the first test to 4.7.   More test data could be

obtained at ΔK's between 40 and 50 MPa√m if longer tests (several days)

were conducted.   Crack closure was not a problem during these tests due

to the high fracture toughness of EX-00053 at 300°C.

X-2M: Both tests on X-2M showed consistent results (see Figure 32)

with an m value of 6.0 for the combined tests. K_{max} values of 46.5 and 52.1

MPa√m are about 75-80 percent of the K_{Ic} (63.5 MPa√m) observed during the

static tests at 300°C.   The data, however, are well within the region

associated with stable crack growth.

Combined Data: The data from all of the tests are displayed in

Figure 33.   Although the data points for 8620 span the entire length of
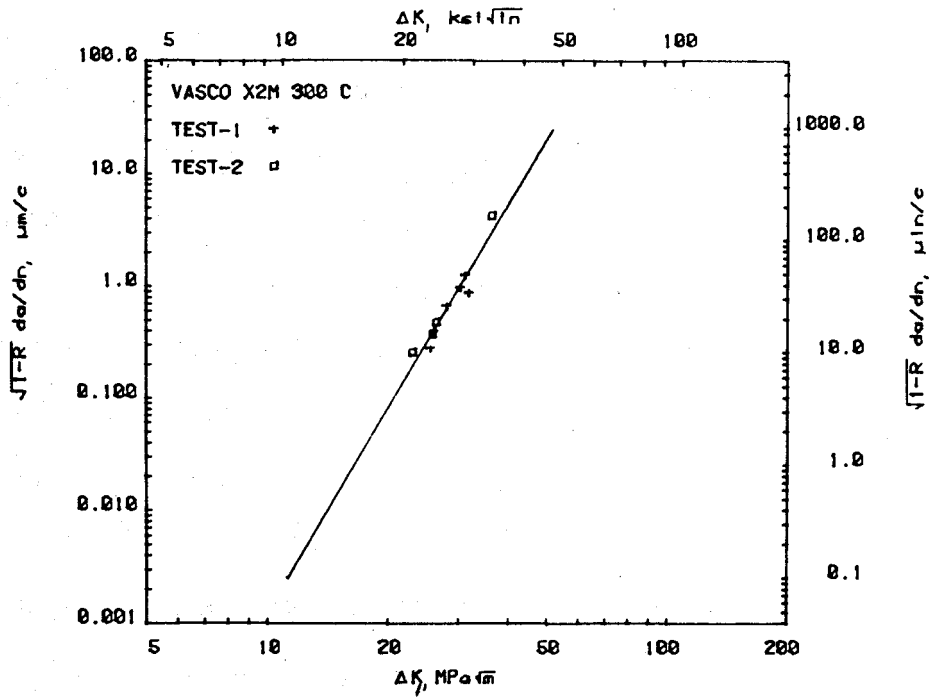
Figure 32. Crack growth rate as a function of stress intensity
factor for X-2M.
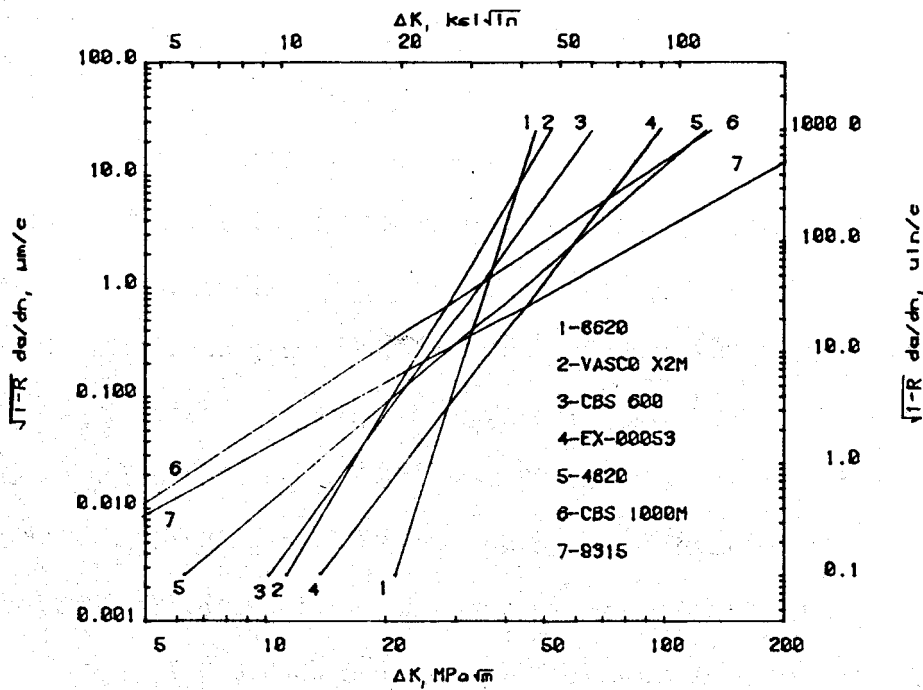
Figure 33. Crack growth rate as a function of stress intensity factor for
all steels tested. (Note that 4820, 8620 and 9315 were tested
at 23°C while CBS 600, CBS 1000M, EX-00053 and X-2M were tested
at 300°C.

the line, it must be emphasized that the other lines are simply extrapolations from the data at low and high ΔK values. As has been previously discussed, the data may not form a straight line in these regions depending on where crack propagation begins and catastrophic failure starts.

Obviously, the best way to evaluate the data is to pick the ΔK range associated with geothermal or conventional drilling. Unfortunately, the ΔK range to which the bits are presently subjected is not known. An alternative method of evaluation would be to pick a crack growth rate, below the critical rate for catastrophic failure, and observe the ΔK at which the rate occurs in an individual steel. The latter approach is a better method for comparing the steels in the test program since a crack growth rate can be picked within the experimental data of all of the steels.

If the steels in Figure 33 are compared at a growth rate ($\sqrt{1-R}$ da/dN) of 0.1 µm/cycle, EX-00053 and 8620 would clearly have the highest ΔK (30 MPa$\sqrt{m}$) while X-2M, CBS 600 and 4820 would be intermediate (20 MPa$\sqrt{m}$) and 9315 and CBS 1000M would display this growth rate at ΔK's of approximately 15 MPa$\sqrt{m}$. If, alternatively, the steels are compared at a growth rate of 1.0 µm/cycle then 9315, EX-00053 and 4820 display the highest ΔK's (40-50 MPa$\sqrt{m}$) while 8620, CBS 1000M and CBS 600 have the same growth rate at a ΔK of 35 MPa$\sqrt{m}$ and X-2M at 30 MPa$\sqrt{m}$. The ΔK of interest is obviously critical since at a stress intensity level of 30 MPa$\sqrt{m}$, 8620 and EX-00053 have crack growth rates an order of magnitude slower than 9315 and CBS 1000M. At a ΔK of 50 MPa$\sqrt{m}$, however, the crack propagation rate in 9315, EX-00053 and 4820 is at least an order of magnitude slower than 8620 and X-2M.

The data generated suggest a wide variation in the room-temperature fatigue behavior of 4820, 8620 and 9315 which is not completely under-

stood at this time. The 300°C fatigue crack resistance data for the high wear resistant steels are certainly within the scatter of the conventional steels at room temperature. It would appear that all of the steels will display adequate fatigue crack resistance when used at elevated temperature, based on the infrequent fatigue failures experienced by 4820, 8620 and 9315 in drill bits. Based on the limited testing performed, EX-00053 appears to show improved fatigue crack resistance when compared to CBS 600 and X-2M. It would also appear that EX-00053 is superior to CBS 1000M at ΔK's less than 78-80 MPa$\sqrt{m}$. 8620 is clearly superior to 9315 and 4820 at ΔK's up to 30 MPa$\sqrt{m}$ but 9315 and 4820 could only be used above 40 MPa$\sqrt{m}$ since cracks in 8620 grow catastrophically above this stress intensity.

SEM micrographs displayed in Figures B19 through B32 (see Appendix B) compare the fracture surfaces of fatigued samples to their statically tested counterparts at a corresponding temperature. There were no major differences between the mode of fracture in the static fracture toughness tests and the fatigue crack resistance tests. All samples appear to have failed in a ductile mode caused by microvoid coalescence. Striations are normally not observed in martensitic structures[19] and none were observed on the fractured surfaces of the fatigued samples. The dimples on static tests were consistently larger than the voids on the fatigued surfaces, confirming the much faster speed at which the fracture toughness measurements were made. The reason for the high m value for 8620, in contrast to normal m values for 4820 and 9315, was not explained by the SEM micrographs. Further fatigue testing is needed to clarify the behavior and to quantify differences between the steels.

CONCLUSIONS

1. Both conventional and high wear resistant steels displayed wide varia-
   tions in fracture toughness over the temperature range 23°C to 400°C.
   It is therefore important to characterize the fracture behavior of
   steels in the temperature range of operation.

2. Steels having microstructures of 100 percent tempered martensite
   (CBS 1000M, EX-00053, X-2M and 9315) displayed nearly constant or
   increasing toughness above room temperature, whereas steels containing
   mixed microstructures (4820, 8620 and CBS 600) decreased significantly
   in fracture toughness in the temperature range 23°C to 300°C.

3. EX-00053 and CBS 1000M were the only steels tested which displayed
   significantly higher toughness than 9315 over the entire temperature
   range. 9315 was superior in toughness to 4820 and 8620 over the
   entire temperature range. In the temperature range normally en-
   countered at the Geysers (150-300°C), all of the steels tested have
   toughness at least equivalent to 4820 and 8620. If accelerated bit
   rotation speeds and higher loads are applied to increase penetration
   rates, EX-00053 and CBS 1000M are the two steels most capable of
   withstanding greater impact loading.

4. EX-00053 and CBS 1000M displayed an increase in toughness between
   23°C and 100°C, associated with a brittle-to-ductile fracture transi-
   tion. EX-00053 increased in toughness from 103.6 MPa$\sqrt{m}$ at room tempera-
   ture to 264.6 MPa$\sqrt{m}$ at 100°C.

5. Fatigue crack resistance measurements at 300°C for CBS 600, CBS 1000M,
   EX-00053 and X-2M were well within the scatter in fatigue behavior

observed for 4820, 8620 and 9315 at room temperature. Although the fatigue data for these steels are limited to date, they suggest that all of the steels have enough fatigue crack resistance to withstand present geothermal drilling conditions. EX-00053 has superior fatigue crack resistance at ΔK's less than 50 MPa$\sqrt{m}$ and appears to be the best candidate for use at 300°C. 8620 displayed slower crack propagation rates at ΔK's less than 30 MPa$\sqrt{m}$ when compared to 4820 and 9315 at room temperature, and 9315 is clearly superior above 50 MPa$\sqrt{m}$.

6. Since bit failure is usually associated with wear, it would appear that studies of the hot hardness and wear resistance of these steels should be conducted on a comparable basis. A cost comparison, as well as fabrication considerations (heat treating, machinability, weldability, etc.) is also needed to determine the economic consequences of using high wear resistant steels to obtain improved penetration rates.

REFERENCES

1. Hendrickson, R. R., S. J. Green, A. H. Jones, and R. W. Winzenried, "Full-Scale Laboratory Testing of Experimental Geothermal Rock Bits," Trans. Geothermal Resources Council, 2, p. 267, 1978.

2. Friedman, E. J. and A. El-Sawy, "Prospects for Improvement in Geothermal Well Technology and Their Expected Benefits," HCP/T4014-04, UC-77c, Mitre Corp., McLean, Virginia, 1978.

3. Hendrickson, R. R., A. H. Jones, R. W. Winzenried, and A. B. Maish, "Field Drilling Tests on Improved Geothermal Unsealed Roller-Cone Bits," Terra Tek Report TR 79-57, 1979.

4. Barker, L. M. and W. C. Leslie, "Short Rod K_{Ic} Tests of Several Steels at Temperatures to 700°K", Fracture 1977, ICF 4, Waterloo, Canada, p. 305, 1977.

5. Barker, L. M., "Evaluation of a Simple Method for Measuring Fracture Toughness," Eng. Frac. Mech., 9, p. 361, 1977.

6. Barker, L. M., "Short Rod Measurements of Al_2O_3," Fracture Mechanics of Canada, 3, edited by R. C. Bradt, D.P.H. Hasselman, and F. F. Lange, Plenum Publishing Co., p. 483, 1978.

7. Barker, L. M., "Theory for Determining K_{Ic} from Small, Non-LEFM Specimens, Supported by Experiments on Aluminum," Int. J. of Fracture, 15, 6, p. 515, 1979.

8. Barker, L. M. and F. I. Baratta, "Comparisons of Fracture Toughness Measurements by the Short Rod and ASTM Standard Method of Test for Plain Strain Fracture Toughness of Metallic Materials (E 399-78)", J. of Testing and Evaluation, 8, 3, p. 97, 1980.

9. Beech, J. F. and A. R. Ingraffea, "Three-Dimensional Finite Element Calibration of the Short Rod Specimen," Geotechnical Engineering Report 80-3, Cornell University, Ithaca, New York, 1980.

10. Barker, L. M. and R. V. Guest, "Compliance Calibration of the Short Rod Fracture Toughness Specimen," Terra Tek Report TR 78-20, 1978.

11. Guest, R. V., "Fracture Toughness Testing Using Short Rod Specimens, Illustrated by Controlled Temperature Tests on M-2 High Speed Tool Steel," to appear in Proceedings of the Symposium on New Developments in Processing and Properties of High Speed Tool Steels, AIME Annual Meeting, Las Vegas, Nevada, February 24-28, 1980. Also, Terra Tek Report TR 80-38, 1980.

12. Barker, L. M., "Residual Stress Effects on Fracture Toughness Measurements," Terra Tek Report TR 80-37, 1980.

13. Shin, T. T. and R. P. Wei, "A Study of Crack Closure in Fatigue," Eng. Frac. Mech., $\underline{6}$, 19, 1974.

14. Paris, P. C., "The Fracture Mechanics Approach to Fatigue," Proc. 10th Sagamore Conference, Syracuse University Press.

15. Hudson, C. M. and H. F. Hardrath, "Effects of Changing Stress Amplitude on the Rate of Fatigue Crack Propagation in Two Aluminum Alloys," NASA TN D 960, 1961.

16. Sosie, D. F., M. R. Mitchell, and E. M. Caulfield," Fundamentals of Modern Fatigue Analysis," Fracture Control Program Report 26, University of Illinois, 1978.

17. Jatczak, C. F., Private communication with R. Cutler, 1980.

18. Hudson, M. and C. Seward, "Compendium of Sources of Fracture Toughness and Fatigue-Crack Growth Rate for Metallic Alloys," Int. J. of Fracture, $\underline{14}$, 1978.

19. Richards, C. E. and T. C. Lindley, "The Influence of Stress Intensity and Microstructure on Fatigue Crack Propagation in Ferritic Materials," Eng. Frac. Mech., $\underline{2}$, p. 951, 1972.

20. Bucci, R. J., W. G. Clark, and P. C. Paris, "Fatigue Crack Propagation Rates under a Wide Variation of ΔK for an ASTM A517 Grade F(T-1) Steel," Stress Analysis and Growth of Cracks, Proceedings of the 1971 National Symposium on Fracture Mechanics, Part 1, ASTM STP 513, p. 177, 1972.

ACKNOWLEDGMENTS

APPENDIX A

HEAT TREATMENTS AND K_{Ic} DATA

TABLE A1

Brookhaven Geothermal Materials Contract Fracture Toughness Data

Steel Type	Manufacturer's Code	Heat Treatment (see attached sheet)	Cylinder Diameter (inches)	$K_{IC SR}$ (ksi√in)				
				RT	100°C	200°C	300°C	400°C
4820	--	A	2	86.9 · 13.3 (15.4) [5 tests]	71.6 · 2.3 (3.2) [3 tests]	52.0 · 7.1 (13.6) [5 tests]	61.4 · 1.4 (2.2) [3 tests]	--
8620	--	B	2	102.3 · 18.7 (18.7) [4 tests]	90.0 · 6.8 (7.5) [4 tests]	67.0 · 1.2 (1.8) [3 tests]	62.8 · 9.8 (15.6) [4 tests]	--
9315	--	C	1	109.8 · 3.4 (3.1) [3 tests]	98.8 · 4.4 (4.5) [3 tests]	86.8 · 4.4 (5.0) [3 tests]	80.0 · 2.7 (3.4) [4 tests]	86.5 ± 1.0 (1.2%) [3 tests]
CBS 600	3	D	2	140.1 · 1.6 (1.2) [2 tests]	--	--	--	--
CBS 600	600	D	1	94.1 · 1.6 (1.7) [2 tests]	77.8 · 0.5 (0.6) [2 tests]	55.9 · 2.3 (4.1) [2 tests]	53.4 · 1.1 (2.0) [2 tests]	65.2 · 0.8 (1.3%) [2 tests]
CBS 600M	671	E	1	63.1 · 2.9 (4.5) [3 tests]	--	--	--	--
CBS 600M	672	F	1	63.3 · 2.3 (3.6) [3 tests]	--	--	--	--
CBS 600	4	F	2	101.3 · 1.9 (1.9) [3 tests]	--	--	79.0 · 0.0 (0.0%) [2 tests]	--
CBS 1000M	1	G	2	51.9 · 0.8 (1.5) [2 tests]	--	--	72.3 [1 test]	--
CBS 1000M	2	H	2	40.9 · 4.1 (10.0) [2 tests]	44.2 · 3.3 (7.5) [2 tests]	--	51.1 [1 test]	--
CBS 1000M	1000-2	I	1	64.5 · 0.1 (0.1) [2 tests]	114.4 · 6.7 (5.9%) [2 tests]	96.05 · 3.9 (4.1%) [2 tests]	92.7 · 1.7 (1.8%) [2 tests]	97.5 · 0.7 (0.7%) [2 tests]
CBS 1000M	3A	J	1	65.3 · 2.4 (3.7) [2 tests]	103.2 · 5.9 (5.7) [2 tests]	92.1 · 2.1 (2.3%) [2 tests]	82.9 · 2.6 (3.2%) [2 tests]	--
CBS 1000M	3B	K	1	56.7 · 0.1 (0.1) [2 tests]	118.9 · 1.7 (1.4) [2 tests]	116.5 · 3.7 (3.2%) [2 tests]	98.3 · 0.4 (0.4%) [2 tests]	--
EX-00053	--	L	2	94.2 · 7.5 (8.0%) [2 tests]	240.5 [2nd test was 268.5 but was invalid-- too much plasticity]	201.2 · 2.1 (1.0) [2 tests]	152.9 · 3.3 (2.1%) [2 tests]	[1 test gave 185.2 but was invalid-- too much plasticity]
VASCO X-2M	--	M	2	43.7 · 2.1 (4.9) [2 tests]	57.7 · 0.8 (1.3%) [2 tests]	60.7 · 1.3 (2.2%) [2 tests]	57.7 · 2.7 (4.7%) [2 tests]	55.0 · 1.5 (2.7%) [2 tests]

61

HEAT TREATMENTS

Code	Procedure

A
1. Pseudo carburized in stainless steel envelope for seven hours at 1700°F (925°C). Air cooled.
2. Austenitized at 1525°F (830°C) for one hour. Water quenched with rigorous agitation.
3. Immediately tempered at 450°F (230°C) for two hours.

B
1. Pseudo carburized in stainless steel envelope for seven hours at 1700°F (925°C). Air cooled.
2. Austenitized at 1560°F (850°C) for one hour. Water quenched with rigorous agitation.
3. Immediately tempered at 450°F (230°C) for two hours.

C
1. Pseudo carburized for seven hours at 1700°F (925°C) in stainless steel envelope and oil quenched after withdrawal from envelope.
2. Reheated to 1500°F (815°C) and held for 30 minutes. Oil quenched.
3. Double tempered at 350°F (175°C) for two hours each cycle.

D
1. Pseudo carburized for seven hours at 1700°F (925°C) in stainless steel envelope and oil quenched after withdrawal from envelope.
2. Conditioned at 1200°F (650°C) for two hours.
3. Reheated in salt to 1535°F (835°C), held 25 minutes (1+30 min. total time) and oil quenched with vigorous agitation.
4. Double tempered at 600°F (315°C) for two hours each cycle.

E
1. Pseudo carburized seven hours at 1700°F (925°C) in stainless steel envelope and oil quenched after withdrawal from envelope.
2. Conditioned at 1200°F (650°C) for four hours.
3. Reheated to 1550°F (845°C) and held for 30 minutes. Oil quenched.
4. Cold treated at -120°F (-85°C) for two hours.
5. Double tempered at 600°F (315°C) for two hours each cycle.

F
1. Pseudo carburized for seven hours at 1700°F (925°C) in stainless steel envelope and oil quenched after withdrawal from envelope.
2. Conditioned at 1200°F (650°F) for two hours.
3. Reheated in salt to 1600°F (870°C) and held 25 minutes (1+30 min. total time). Oil quenched with vigorous agitation.
4. Double tempered at 600°F (315°C) for two hours each cycle.

G
1. Preoxidized at 1700°F (925°C) for 0.5 hour.
2. Pseudo carburized for seven hours at 1700°F (925°C) in stainless steel envelope and oil quenched after withdrawal from envelope.
3. Conditioned at 1200°F (650°C) for two hours.
4. Reheated to 1750°F (955°C) for 25 minutes at heat (1+45 total time) in a stainless steel wrap and oil quenched.
5. Cold treated at -120°F (-84°C) for three hours.
6. Double tempered at 600°F (315°C) for two hours each cycle.

APPENDIX B

SEM MICROGRAPHS

Code	Procedure

H
1. Preoxidized at 1700°F (925°C) for 0.5 hours.
2. Pseudo carburized for seven hours at 1700°F (925°C) in stainless steel envelope and oil quenched after withdrawal from envelope.
3. Conditioned at 1200°F (650°C) for two hours.
4. Reheated in individual stainless wrap to 1550°F (815°C) for 30 minutes at heat, then heated to 2000°F (1090°C) and held for 10 minutes. Oil quenched.
5. Stress relieved at 700°F (370°C) for one hour.
6. Triple tempered at 1000°F (535°C) for two hours each cycle.

I
1. Pseudo carburized at 1700°F (925°C) in stainless steel envelope and oil quenched after withdrawal from envelope.
2. Reheated to 1750°F (955°C) and held for 30 minutes. Oil quenched.
3. Cold treated at -120°F (-85°C) for two hours.
4. Double tempered at 600°F (315°C) for two hours each cycle.

J
1. Pseudo carburized at 1700°F (925°C) in stainless steel envelope and oil quenched after withdrawal from envelope.
2. Conditioned at 1200°F (650°C) for four hours.
3. Reheated to 1675°F (915°C) and held for 30 minutes.
4. Cold treated at -120°F (-85°C) for two hours.
5. Double tempered at 600°F (315°C) for two hours each cycle.

K.
Same as J except tempered at 800°F (425°C) for two hours each cycle.

L.
1. Pseudo carburized in stainless steel envelope for seven hours at 1700°F (925°C). Air cooled.
2. Austenitized at 1675°F (910°C) for one hour. Oil quenched with rigorous agitation.
3. Tempered at 800°F (425°C) for one hour.

M.
1. Pseudo carburized in stainless steel envelope for two hours at 1850°F (1010°C). Air cooled.
2. Austenitized at 2050°F (1120°C) for 20 minutes. Air cooled.
3. Double tempered at 600°F (315°C) for two hours each cycle.
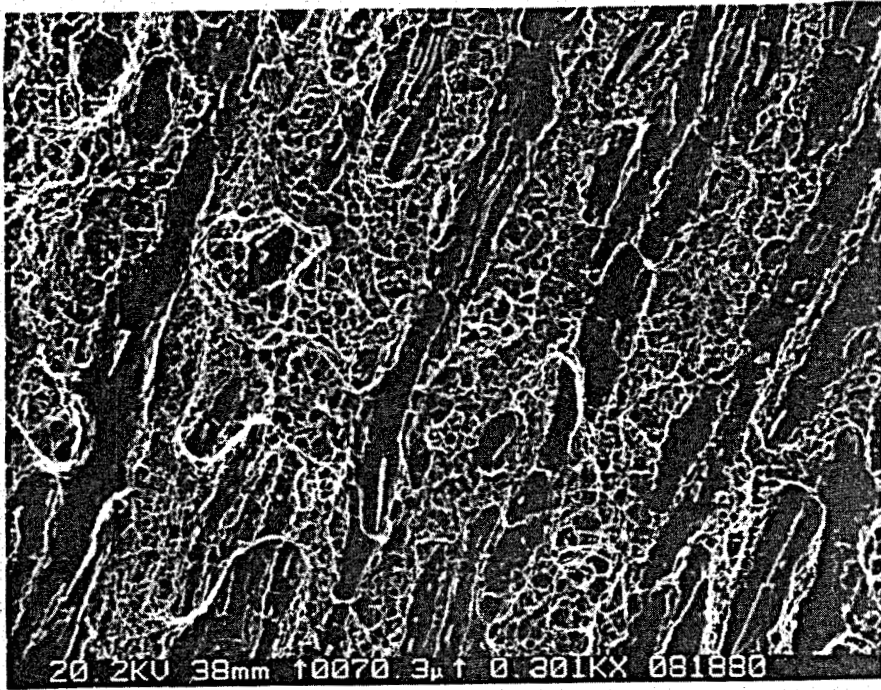
Figure B1. AISI 4820. Room Temperature Static Test.
Ductile Fracture (300X).
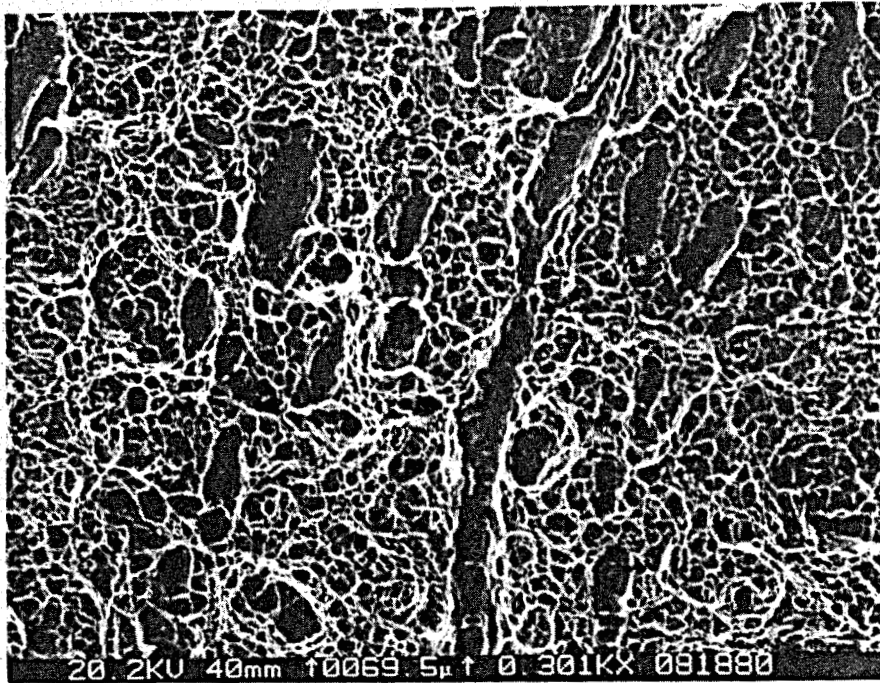
Figure B2. AISI 4820. 300°C Static Test. Ductile
Fracture (300X).

67
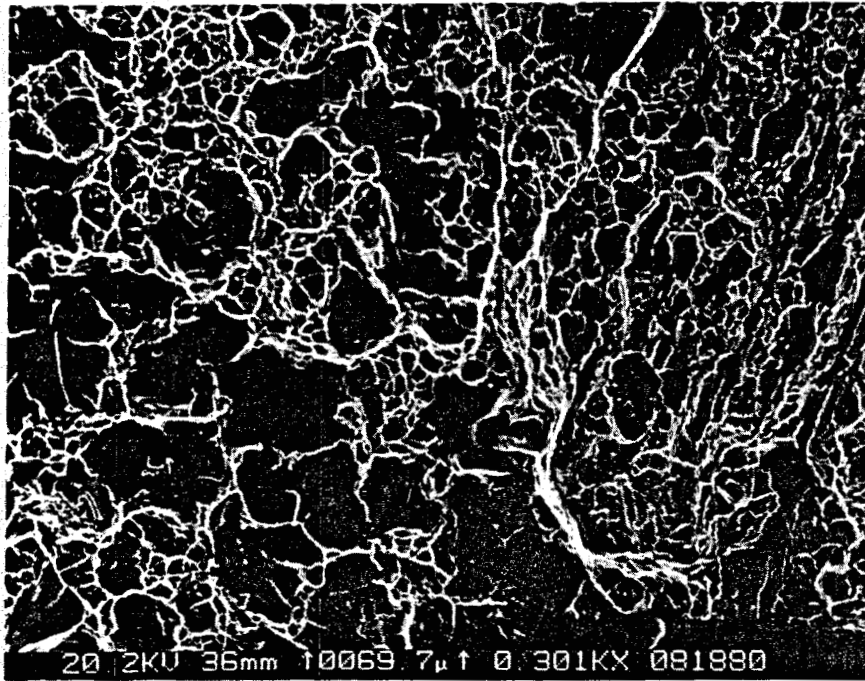
Figure B3. AISI 8620. Room Temperature Static Test.
25-75% Brittle Cleavage (300X).
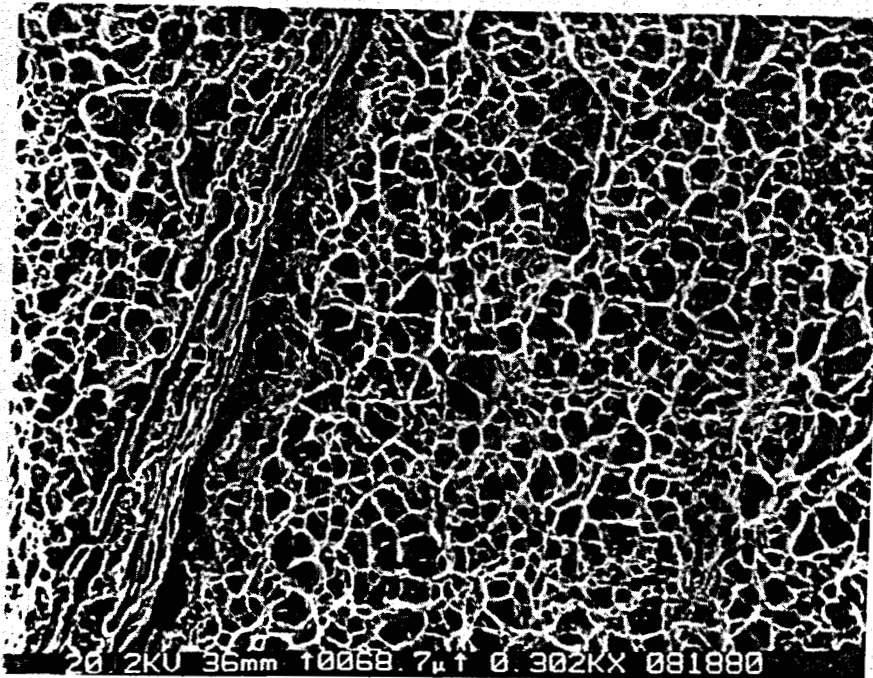
Figure B4. AISI 8620. 300°C Static Test. Ductile
Fracture (300X).
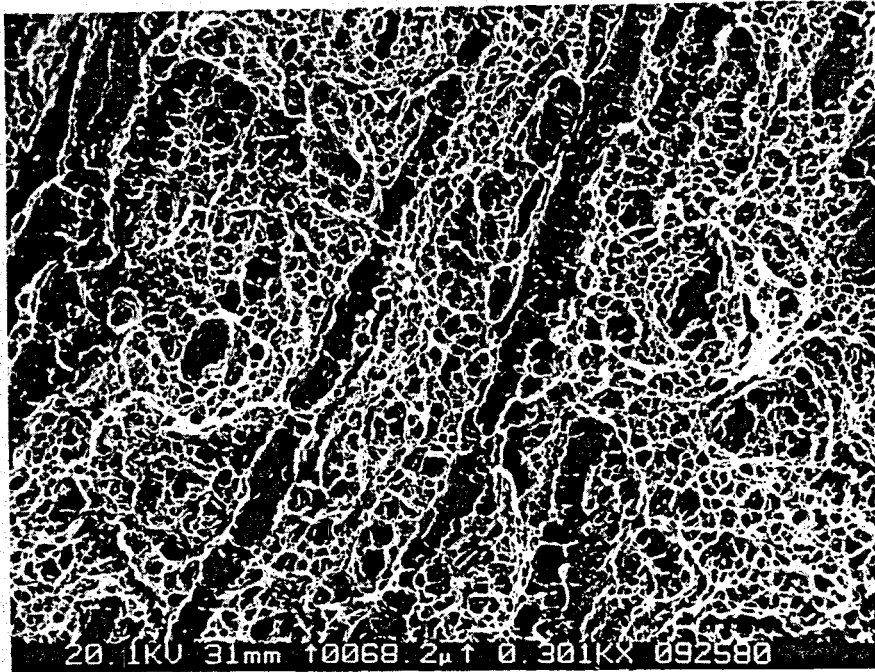
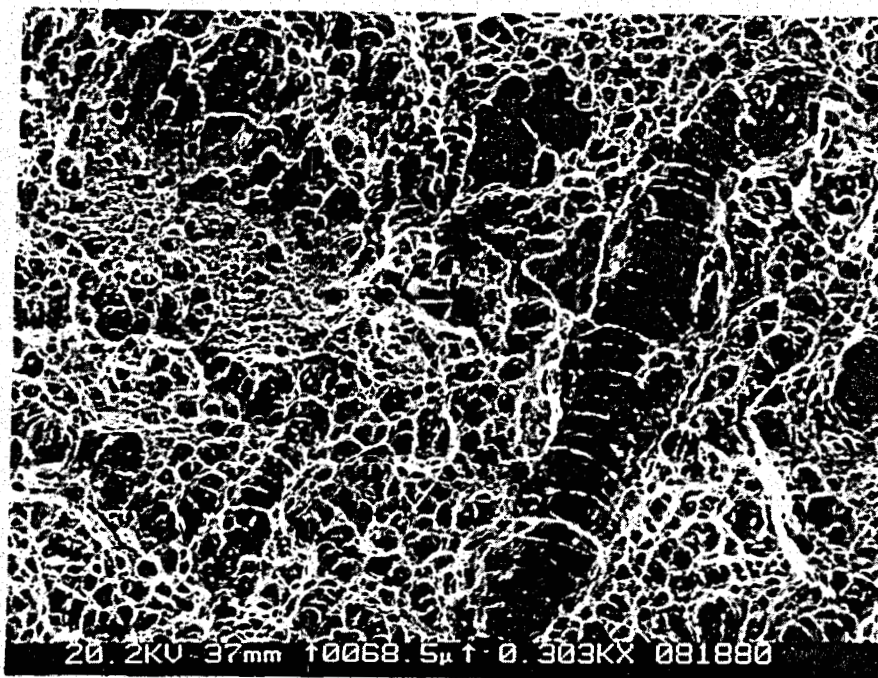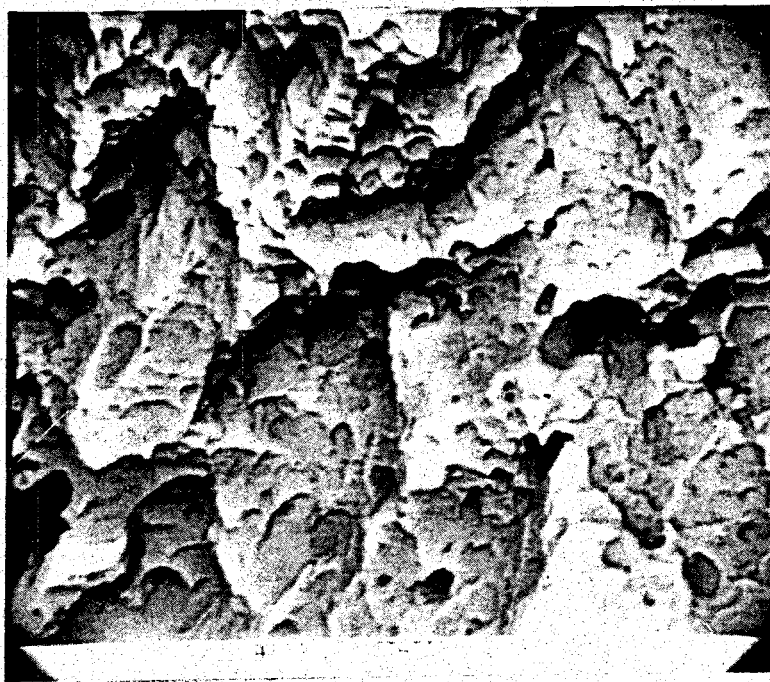Figure B5.   AISI 9315.   Room Temperature Static Test.
Ductile Fracture (300X).
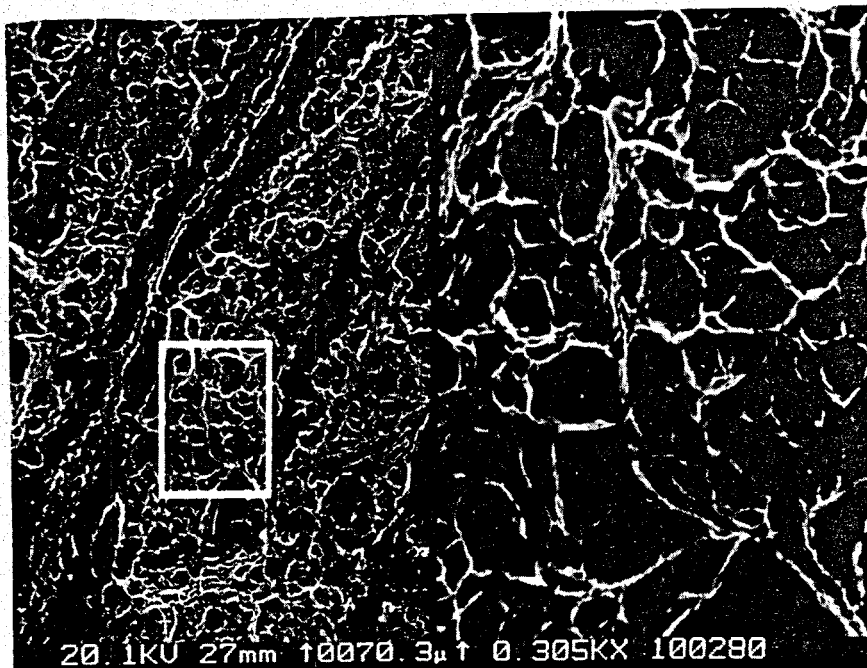
Figure B6.   AISI 9315.   100°C Static Test.   Ductile
Fracture (300-1200X).
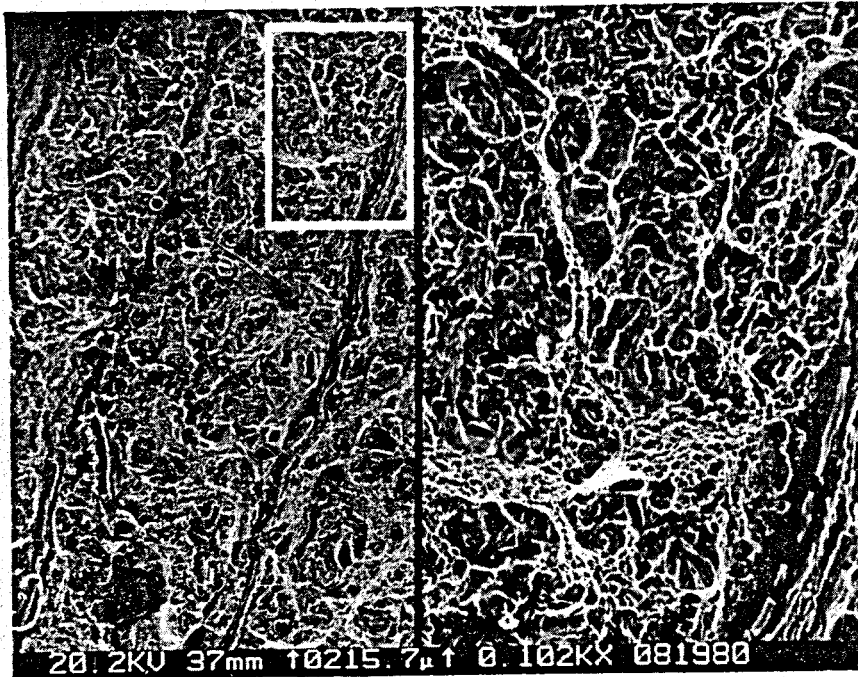
Figure B7. CBS 600 (Heat Treatment F). Room Temperature
Static Test. Ductile Fracture (100-300X).
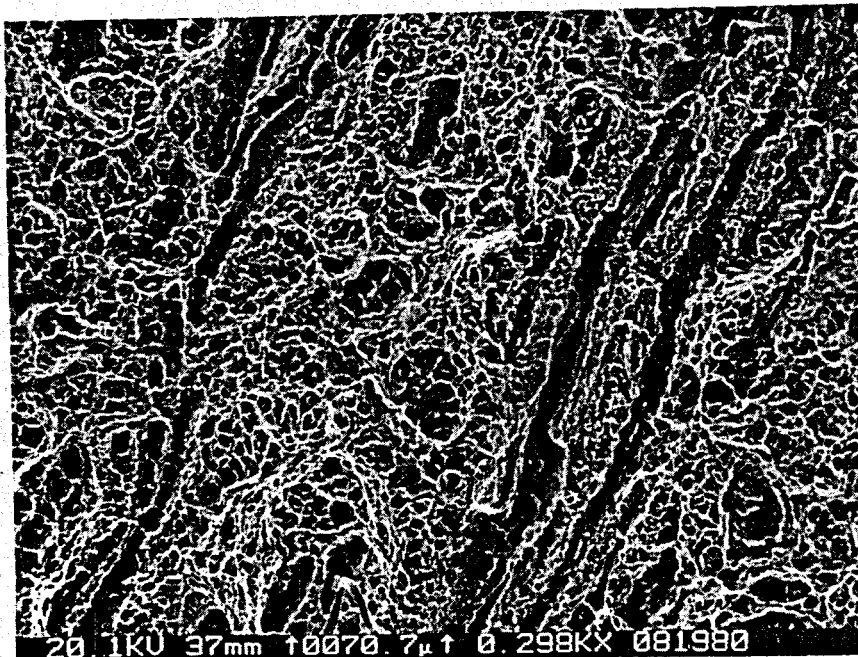
Figure B8. CBS 600 (Heat Treatment D). Room Temperature
Static Test. Ductile Fracture (300X).
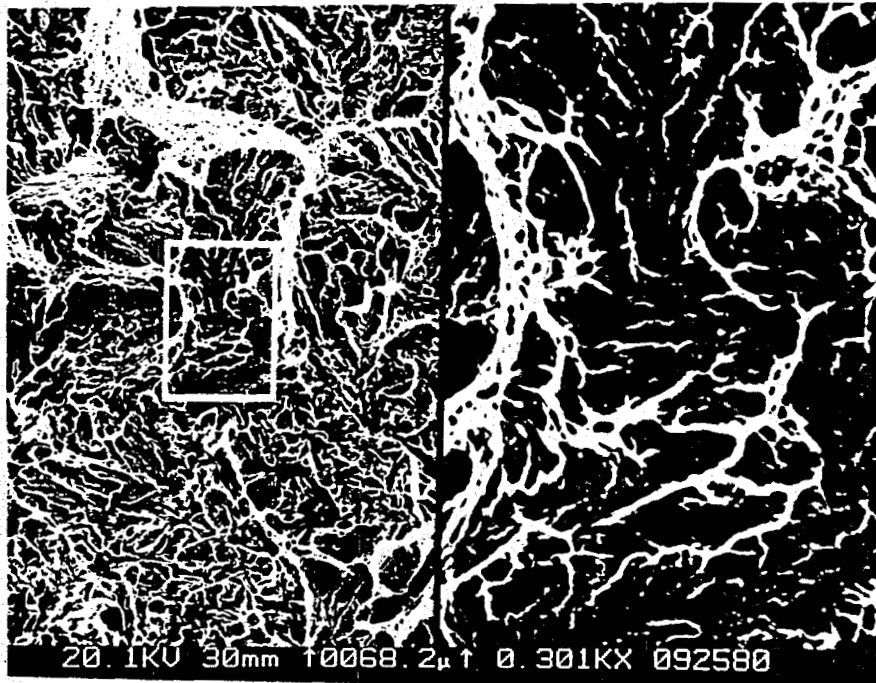
Figure B9. CBS 1000M (Heat Treatment I). Room Temperature Static
Test. 25-75% Brittle Cleavage (300-1200X).
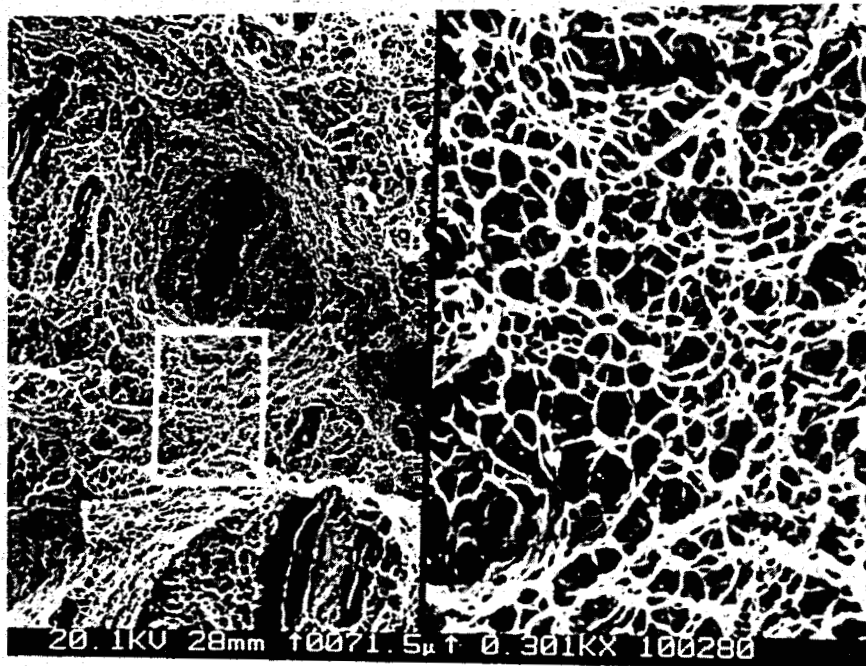
Figure B10. CBS 1000M (Heat Treatment I). 100°C Static Test.
Ductile Fracture (300-1200X).
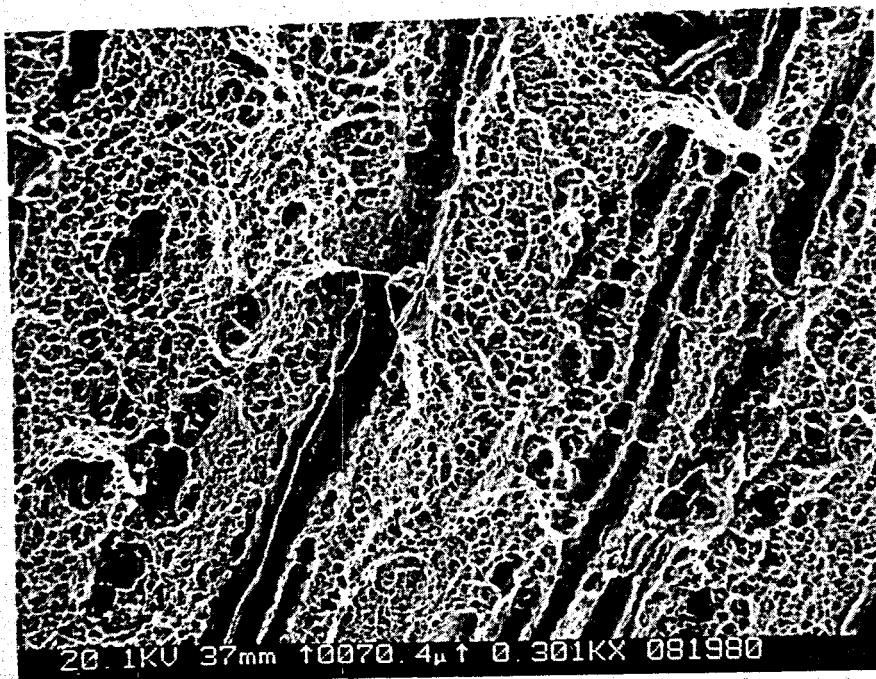
Figure B11. CBS 1000M (Heat Treatment I). 300°C Static Test.
Ductile Fracture (300X).
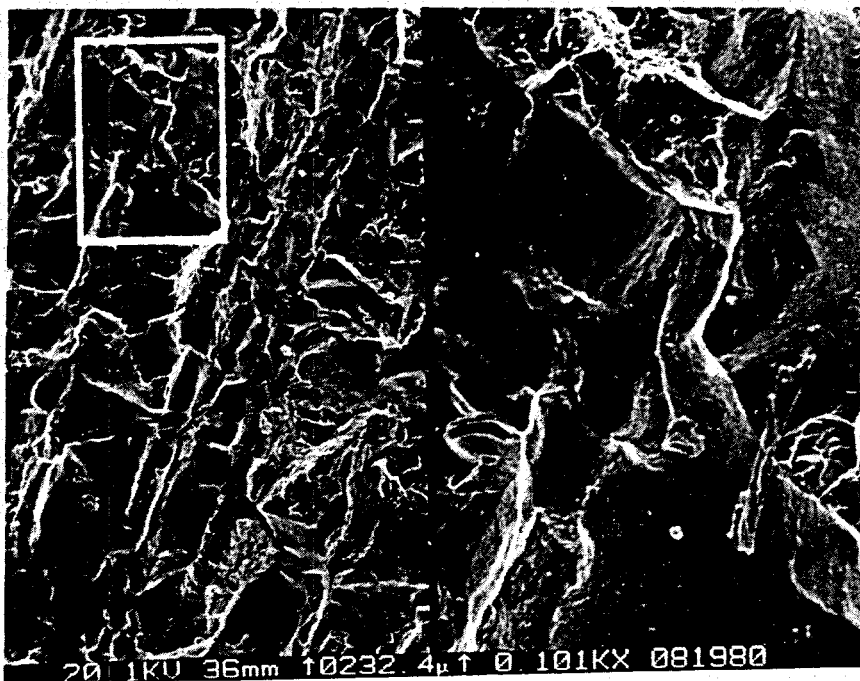
Figure B12. CBS 1000M (Heat Treatment H). Room Temperature
Static Test. Brittle Cleavage (300X).
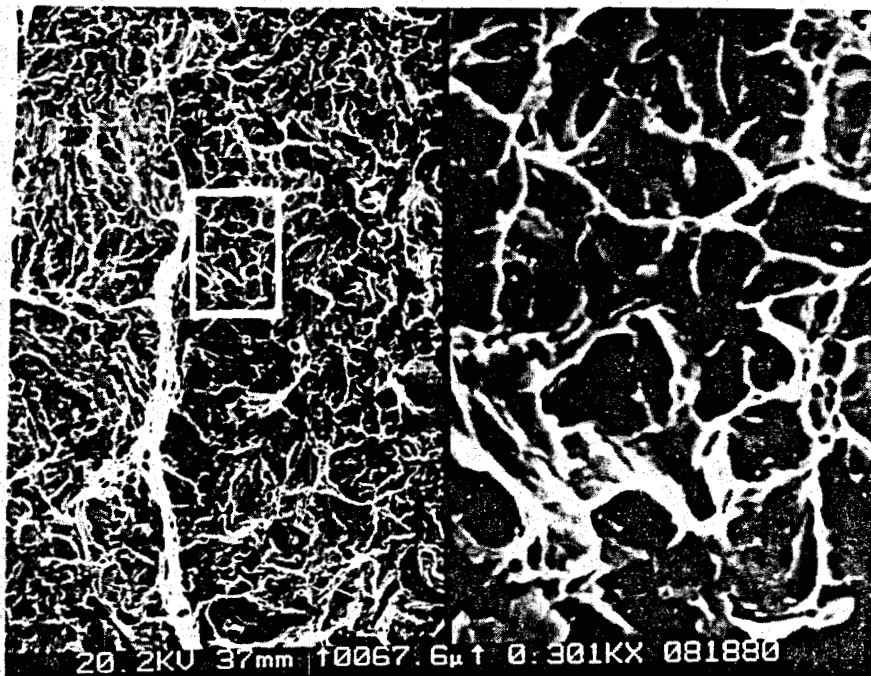
Figure B13. EX-00053. Room Temperature Static Test.
Less than 25% Brittle Cleavage (300-1500X).

Figure B14. EX-00053. 100°C Static Test. Ductile
Fracture (300X).
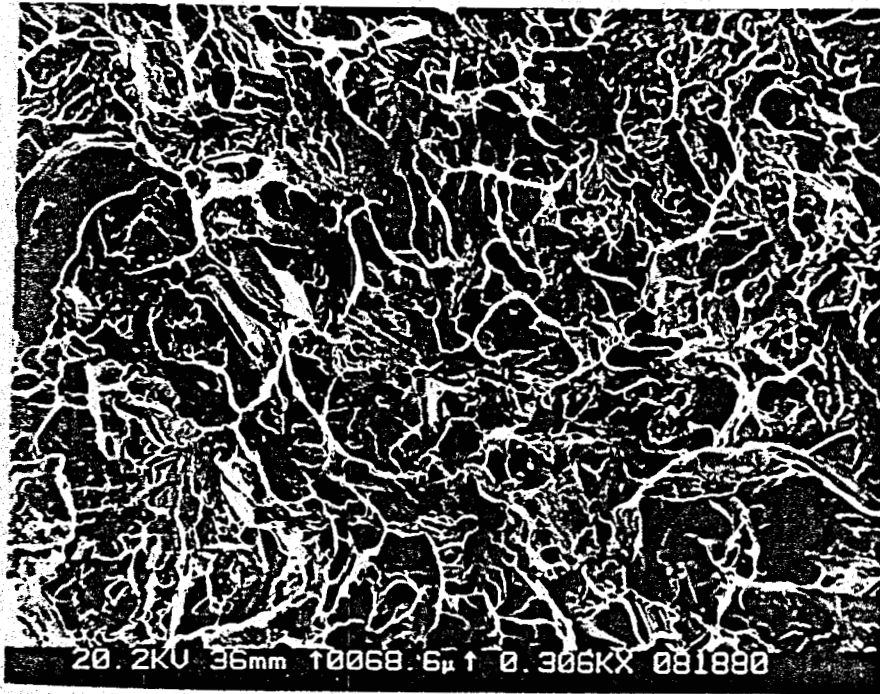
Figure B15. Vasco X2M. Room Temperature Static Test.
Brittle Cleavage (300X).
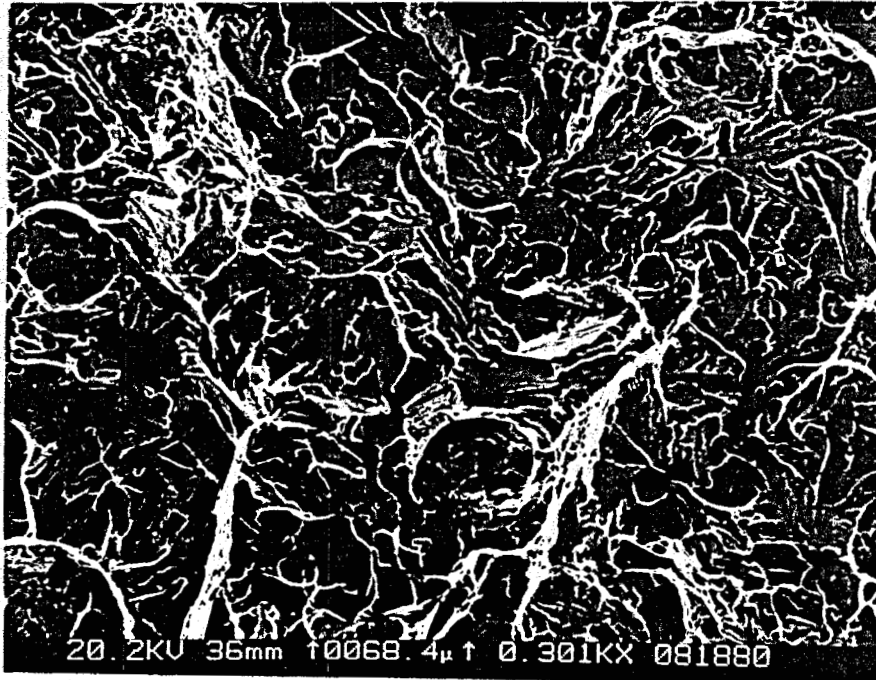
Figure B16. Vasco X2M. 100°C Static Test. Brittle
Cleavage (300X).
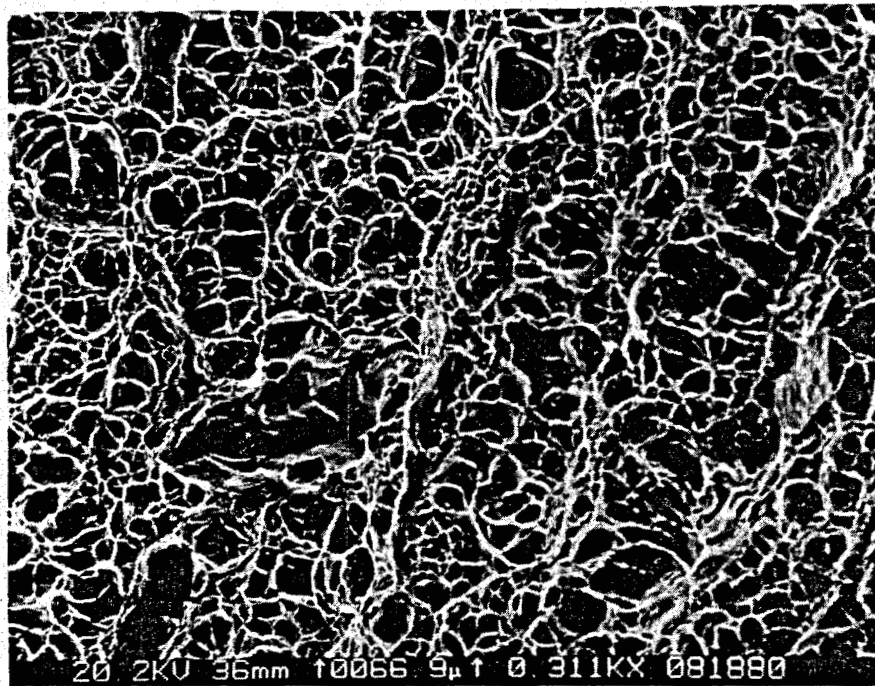
Figure B17. Vasco X2M. 200°C Static Test. Less than 25% Brittle Cleavage (300X).
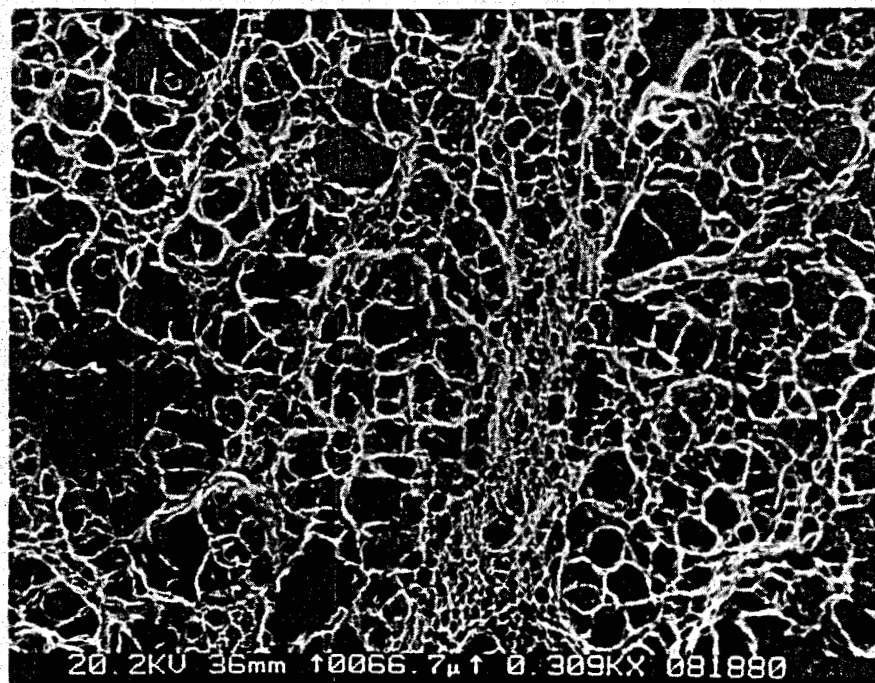
Figure B18. Vasco X2M. 300°C Static Test. Ductile Fracture (300X).

Figure B19.   AISI 4820.   Room Temperature Fatigue Test (1900X).

Figure B20.   AISI 4820.   Room Temperature Static Test (1900X).
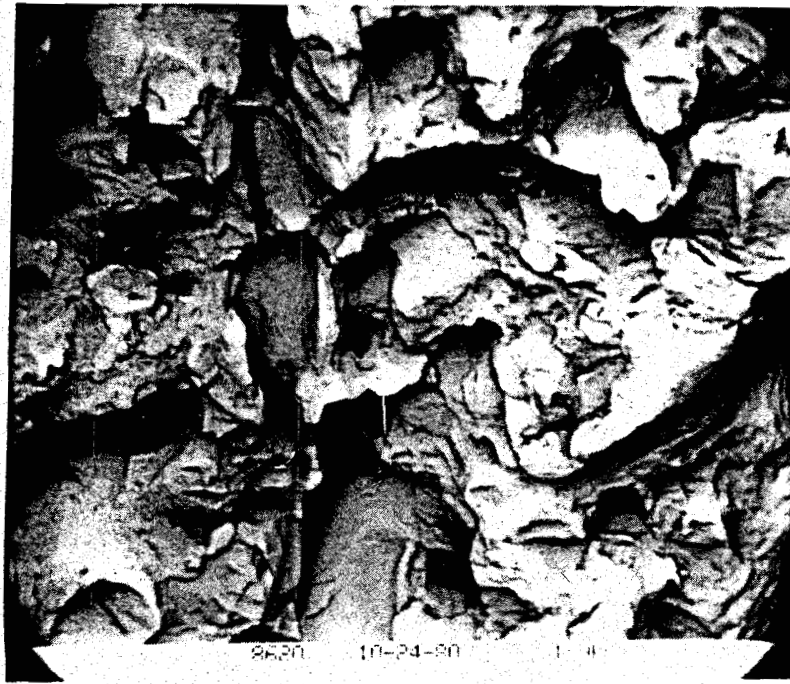
Figure B21. AISI 8620. Room Temperature Fatigue Test (1900X).
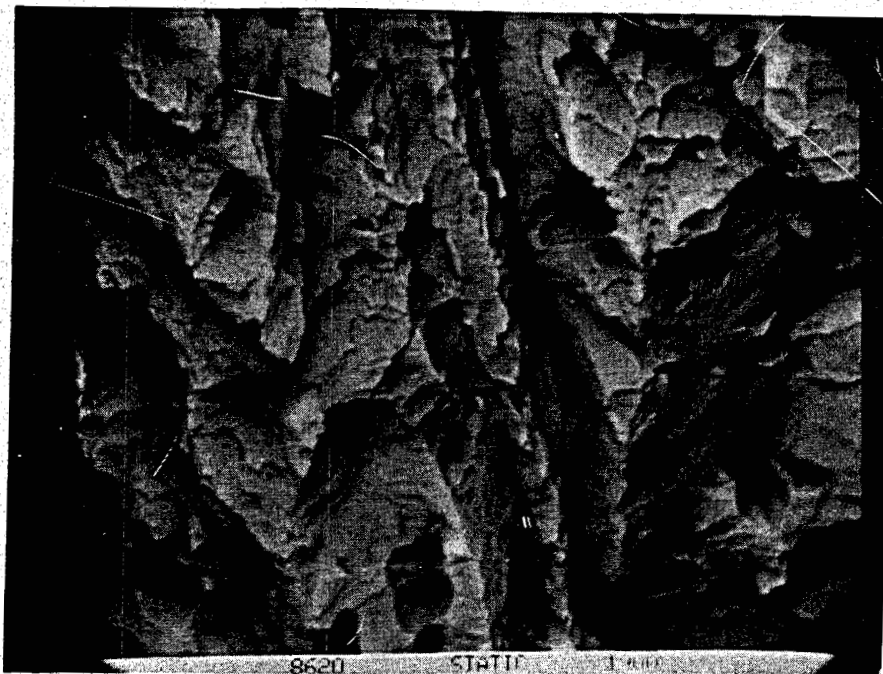
Figure B22. AISI 8620. Room Temperature Static Test (1900X).

Figure B23. AISI 9315. Room Temperature Fatigue Test (1750X).
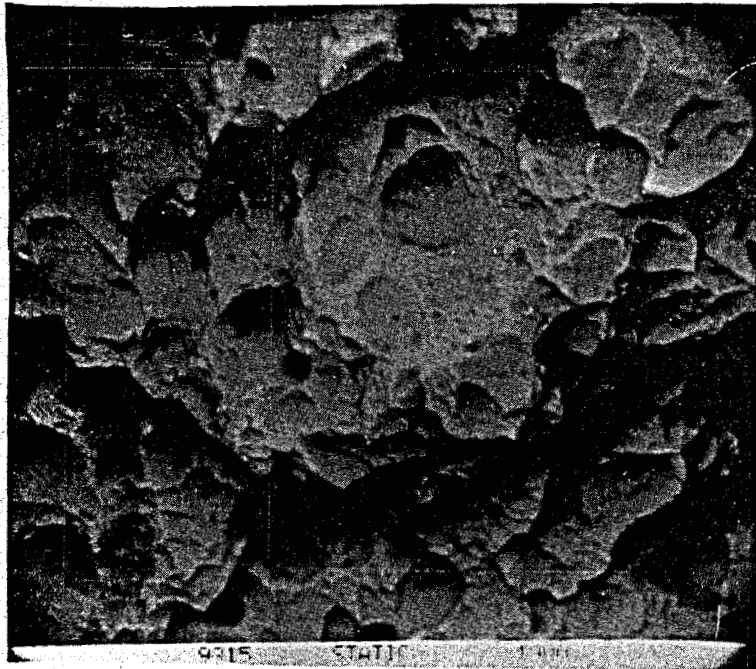
Figure B24. AISI 9315. Room Temperature Static Test (1900X).
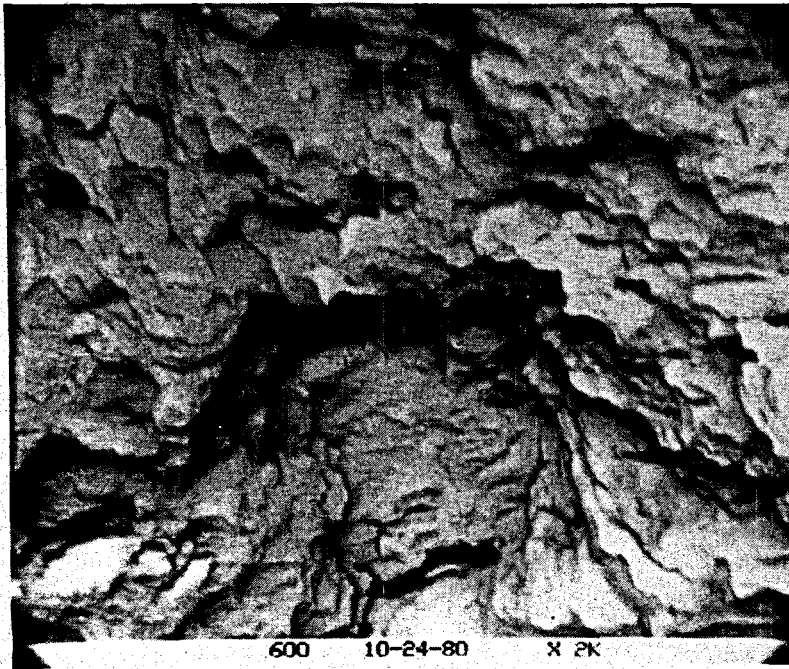
Figure B25.   CBS 600 (Heat Treatment D).   300°C Fatigue Test (2000X).
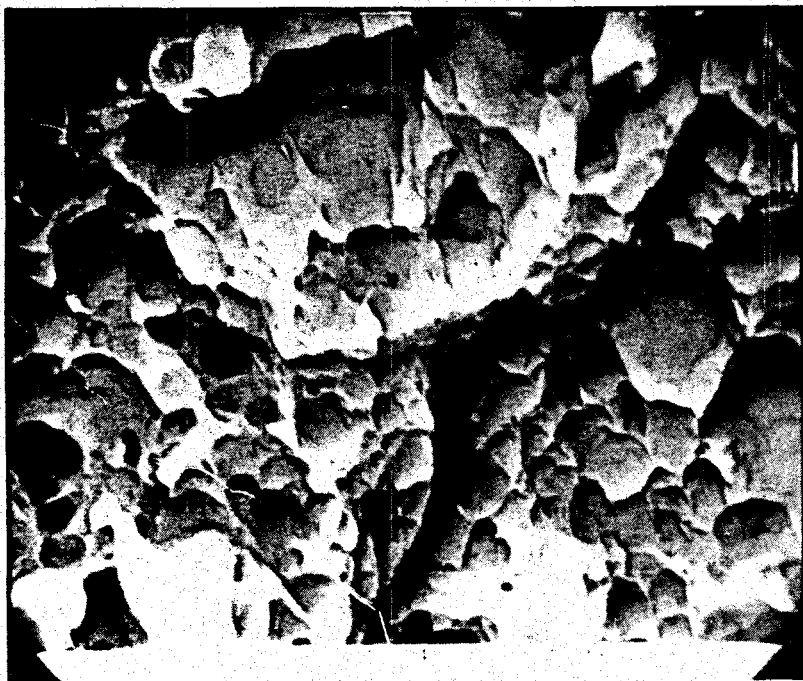
Figure B26.   CBS 600 (Heat Treatment D).   300°C Static Test (1850X).
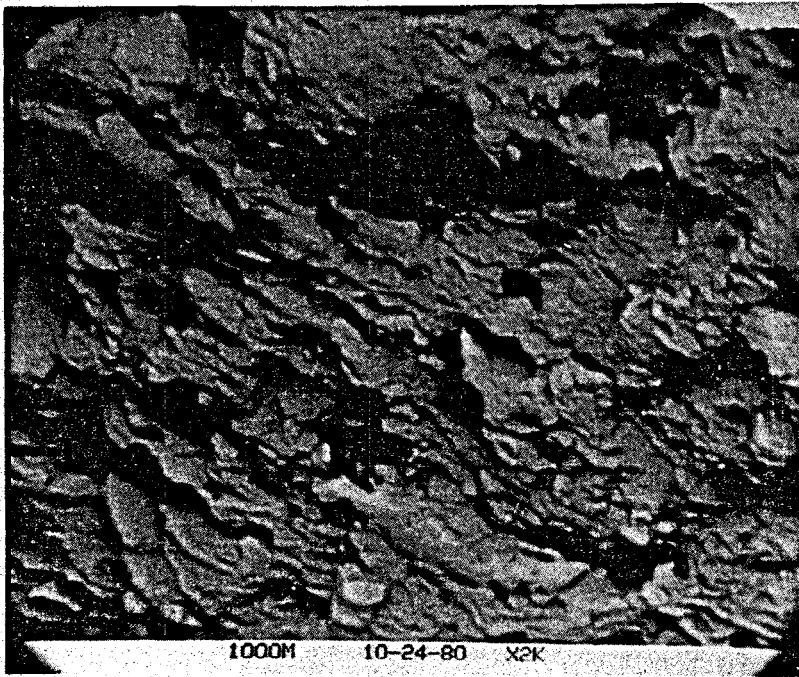
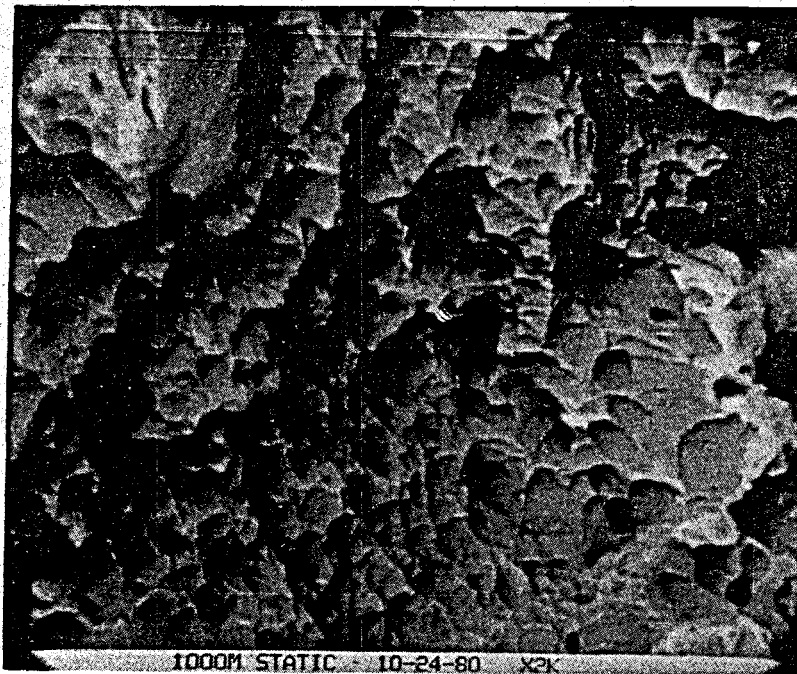Figure B27. CBS 1000M (Heat Treatment G). 300°C Fatigue Test (2000X).

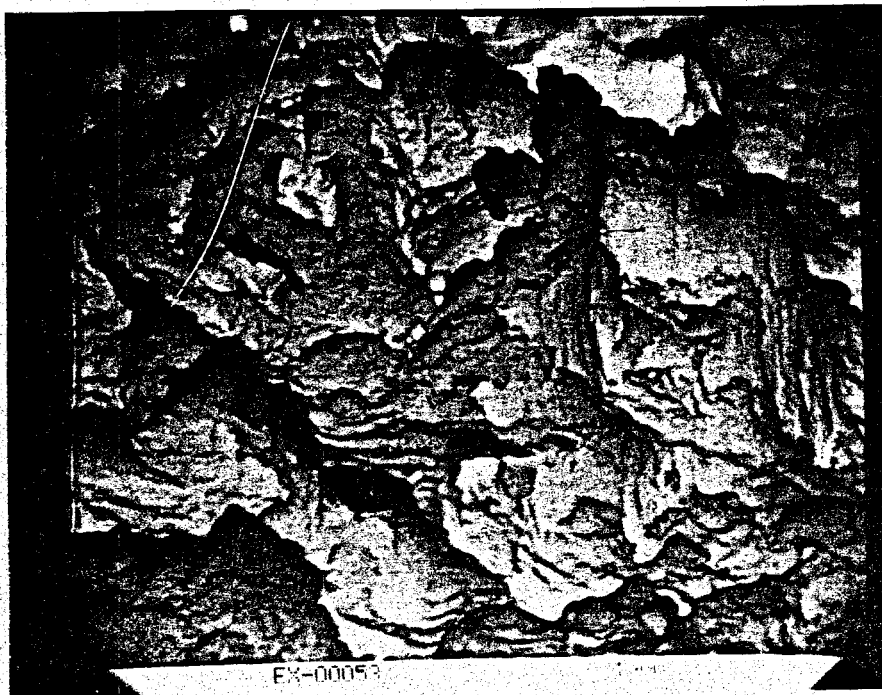Figure B28. CBS 1000M (Heat Treatment G). 300°C Static Test (2000X).

Figure B29. EX-00053. 300°C Fatigue Test (1900X).
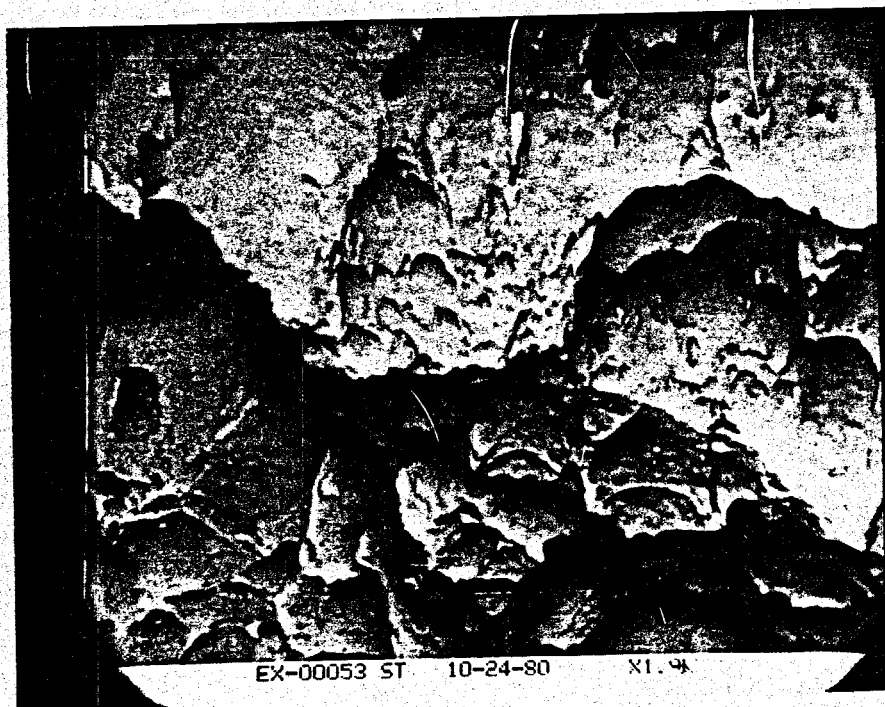

Figure B30. EX-00053. 300°C Static Test (1900X).
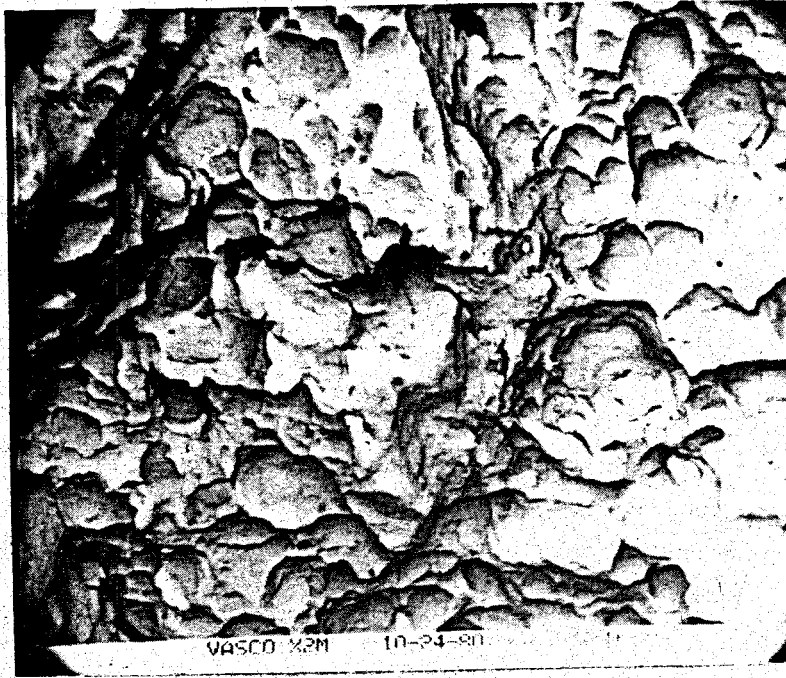
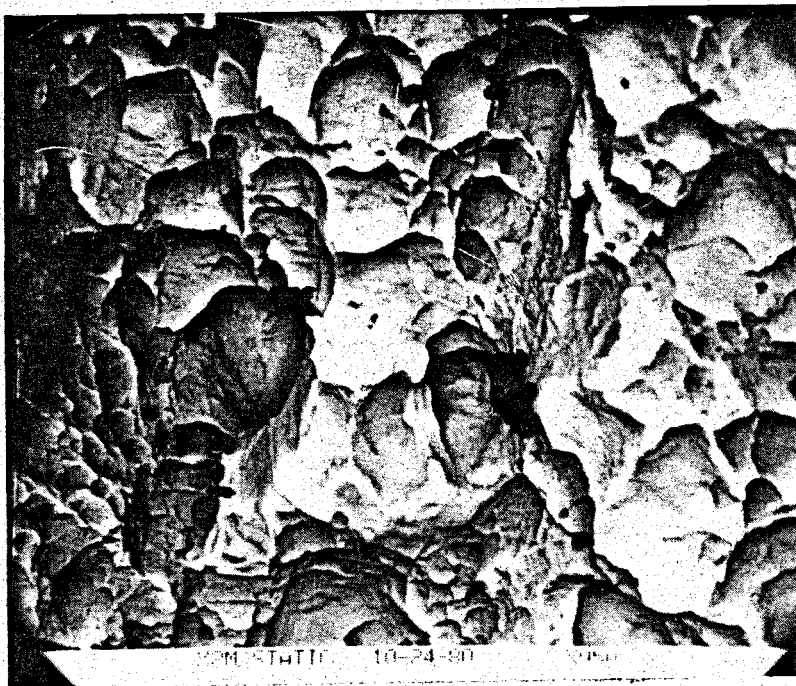Figure B31.   Vasco X2M.   300°C Fatigue Test (1000X).

Figure B32.   Vasco X2M.   300°C Static Test (950X).

APPENDIX C

PROGRAM PARTICIPANTS

CBS Steels

Timken Company
3901 MacArthur Boulevard
Suite 104
Newport Beach, California   92660
(714) 955-1700
Paul Garmus

Timken Research Center
1835 Deuber S.W.
Canton, Ohio   44706
(216) 497-2009
Chester F. Jatczak

EX-00053

Carpenter Technology Corporation
Carpenter Steel Division
P.O. Box 662
Reading, Pennsylvania   19603
(215) 371-2000
Walter E. Burd

Vasco X2M

Teledyne/Vasco
P.O. Box 151
Latrobe, Pennsylvania   15650
(412) 537-5551
Richard J. Henry